Salivary proteins of *Phloeomyzus passerinii*, a plant-manipulating aphid, and their impact on early gene responses of susceptible and resistant poplar genotypes

Luis Portillo Lemus [1, 2] *, Jessy Tricard [1, 2] *, Jérôme Duclercq [2], Quentin Coulette [2], David Giron [3], Christophe Hano [1], Elisabeth Huguet [3], Frédéric Lamblin [1], Anas Cherqui [2] °, Aurélien Sallé [1] °†

[1] Laboratoire de Biologie des Ligneux et des Grandes Cultures, INRA, Université d'Orléans, 45067, Orléans, France

[2] Ecologie et Dynamique des Systèmes Anthropisés, EDYSAN UMR CNRS-UPJV 7058, Université de Picardie Jules Verne, Amiens, France

[3] Institut de Recherche sur la Biologie de l'Insecte, UMR 7261, CNRS/Université François-Rabelais de Tours, Tours, France

* L. Portillo Lemus and J. Tricard should be considered joint first author

° A. Cherqui and A. Sallé should be considered joint senior author

† corresponding author

Declarations of interest: none

Authors' contribution

- AC, AS and DG conceived the ideas. JD, AC and AS designed methodology. LPL, JD and FL collected the plant-related data. JT, QC, CH and EH collected the insect-related data. LPL and JT analyzed the data. AC and AS led the writing of the manuscript. All authors have read and approved the manuscript.

Abstract

Successful plant colonization by parasites requires the circumvention of host defenses, and sometimes a reprogramming of host metabolism, mediated by effector molecules delivered into the host. Using transcriptomic and enzymatic approaches, we characterized salivary glands and saliva of *Phloeomyzus passerinii*, an aphid exhibiting an atypical feeding strategy. Plant genes responses to salivary extracts of *P. passerinii* and *Myzus persicae* were assessed with poplar protoplasts of a susceptible and a resistant genotype, and in a heterologous *Arabidopsis* system. We predict that *P. passerinii* secretes a highly peculiar saliva containing effectors potentially interfering with host defenses, biotic stress signaling and plant metabolism, notably phosphatidylinositol phosphate kinases which seemed specific to *P. passerinii*. Gene expression profiles indicated that salivary extracts of *M. persicae* markedly affected host defenses and biotic stress signaling, while salivary extracts of *P. passerinii* induced only weak responses. The effector-triggered susceptibility was characterized by downregulations of genes involved in cytokinin signaling and auxin homeostasis. This suggests that *P. passerinii* induces an intracellular accumulation of auxin in susceptible host genotypes, which is supported by histochemical assays in *Arabidopsis*. This might in turn affect biotic stress signaling and contribute to host tissue manipulation by the aphid.

Keywords

Effector, effector-triggered susceptibility, *Myzus persicae*, plant-insect interaction, *Populus*, resistance, auxin, cytokinin

45 **1 Introduction**

46

47 In nature, plants engage in multiple interactions with a variety of organisms, resulting in either beneficial
48 or detrimental impacts on plant performance. These interplays are mediated by effectors delivered into
49 the host-plant, either in the apoplast or within plant cells [1, 2]. Effectors can be defined as molecules
50 secreted by plant-associated organisms that alter host cell structure and function, positively or
51 negatively depending on the partners involved [1]. This can be achieved through a direct modification of
52 host molecules, or of their activity, by effectors with enzymatic or binding activities, or a modification of
53 host gene expression by effectors with a nucleic acid binding activity [3].
54 Within the frame of host-parasite interactions, effectors have evolved to target various host functions
55 and key processes. They primarily aim at suppressing plant immunity [1, 3]. For instance, parasites can
56 target and inactivate plant second messengers involved in stress signaling such as Ca^{2+}, reactive oxygen
57 species (ROS) and extracellular ATP with cation-binding effectors, peroxiredoxins and apyrases,
58 respectively [4, 5]. In some situations, effectors can also alter plant development, and promote the
59 manipulation of plant resources by parasites [1, 3, 6]. For example, several pathogens secrete effectors
60 which induce the production of sugar efflux transporters and hijack host sugars for their own nutrition
61 [7]. Similar reconfiguration of host plant metabolism and tissues, to turn them into optimal substrates
62 for development and fitness, have also been reported in plant pests [e.g. 6, 8, 9]. Successful interactions
63 among parasite effectors and their targets lead to an effector-triggered susceptibility [3]. Nonetheless,
64 resistant plant genotypes have evolved receptors, mostly with nucleotide-binding leucine-rich repeat
65 (NB-LRR), that specifically interact with parasite effectors to induce an effector-triggered immunity [10].
66 Microbial pathogen effectors have been extensively studied [e.g. 11, 12]. Comparatively, effectors of
67 insect herbivores and their impact on host plants have received only a limited attention until recently
68 [13, 14]. Evidence indicates that both effector-triggered susceptibility and immunity also occur in plant-

69 insect interactions [e.g. 15, 16]. Consequently, as for pathogens, a deep mechanistic understanding of
70 effector action, i.e. an identification of effectors involved in the interplay and of their targets in host-
71 plants, would be necessary to develop a sustainable management of agricultural and forestry pests,
72 based on resistant plant genotypes [17].
73 The woolly poplar aphid, *Phloeomyzus passerinii* Sign., is a major pest of poplar plantations in the
74 Mediterranean Basin, the Near East and France [18]. This aphid does not feed on sap but in the cortical
75 parenchyma of its host-trees, where it induces a reaction tissue presumably acting as a physiological
76 sink, draining nutrients from surrounding tissues [18, 19, 20]. During aphid outbreaks, when poplar
77 trunks are covered with aphid colonies, the accumulation of reaction tissues dramatically affects host
78 allocations of non-structural carbohydrates and nitrogen compounds, and infested mature trees can die
79 rapidly, within a few months [18, 21]. Such outbreaks only occur in stands of susceptible poplar
80 genotypes. Detailed histochemical investigations during early stages of infestation have unraveled that
81 tissues affected by the unusually damaging probing activity of *P. passerinii* in these susceptible
82 genotypes exhibit weak defense reactions, with limited lignification and accumulation of phenolic
83 compounds [19, 20]. During later stages, a reaction tissue differentiate in the cortical parenchyma,
84 characterized by an intense cell multiplication and hypertrophy, an accumulation of free and protein-
85 bound amino acids, and an absence of both vacuolar phenolic compounds and starch granules [20, 22].
86 The differentiation of this reaction tissue improves both aphid performance and feeding behavior [23].
87 Conversely, in resistant poplar genotypes, an intense lignification and a marked accumulation of phenolic
88 compounds occur readily after the onset of probing, blocking further differentiation of reaction tissues
89 and preventing aphid colonization [18, 20]. It is therefore likely that *P. passerinii* induces either an
90 effector-triggered susceptibility in susceptible poplar genotypes, allowing a beneficial manipulation of
91 host tissue for the aphid, or a rapid and intense immunity response in resistant poplar genotypes
92 preventing aphid nutrition. In-depth functional approaches would allow to unravel the molecular

93 mechanisms that contribute to either the success or the failure of this pest establishment on its host-
94 plant, which could ultimately help to improve poplar breeding programmes.
95
96 We hypothesize (i) that since it has a peculiar feeding strategy for an aphid [23], and it can hijack and
97 reconfigure the metabolism of its host plant to improve its nutritional value, *P. passerinii* should possess
98 a rich and atypical repertoire of salivary effectors compared to other sap-feeding aphids. Considering
99 that susceptible hosts implement weak defense reactions when infested, we further hypothesize (ii) that
100 salivary effectors successfully alter biotic stress signaling and / or defense molecules in these host
101 genotypes to induce an effector-triggered susceptibility. Alternatively, in resistant hosts, the effector-
102 triggered immunity should lead to a marked upregulation of defense-related genes. Finally, since it can
103 manipulate host metabolism and anatomy, our last hypothesis (iii) is that some of its salivary effectors of
104 *P. passerinii* can target genes involved in the cell-division cycle and / or induce the disruption or diversion
105 of auxin and/or cytokinin-dependent pathways, which are important regulators of plant growth,
106 differentiation and defense [6, 24].
107 More specifically, our first objective was to characterize with transcriptomic and enzymatic approaches
108 the salivary gland encoded proteins and saliva, respectively, of *P. passerinii*. Our second objective was to
109 assess *in vivo*, with a RT-qPCR approach, early responses of poplar genes belonging to different
110 metabolic and signaling pathways using protoplasts exposed to aphid saliva. Protoplasts were used to
111 simulate a host cellular response to salivary effectors of aphids. Our last objective was to investigate the
112 impact of salivary extracts on specific gene expression *in planta*, in a heterologous *Arabidopsis* system.
113 For all these steps comparative approaches were used. The predicted salivary gland encoded proteins of
114 *P. passerinii* were compared with those of a sap-feeding aphid, *Myzus persicae* (Sulzer) [25, 26], in order
115 to identify proteins common to both aphid species as well as proteins specific to *P. passerinii*. To get
116 insight into how *P. passerinii* affects host immune system and metabolism during both an effector-

117 triggered susceptibility and an immune response, the impact of salivary extracts on gene expression
118 were assessed with poplar genotypes either susceptible or resistant to *P. passerinii*. To compare with
119 non-host interactions, the protoplasts of these poplar genotypes were also exposed to salivary extracts
120 of *M. persicae*, which do not feed on poplar.
121
122 **2 Materials and Methods**
123
124 **2.1 Plant and insect material**
125
126 Two aphid species were considered in our study: *P. passerinii*, our model species, and the green peach
127 aphid, *M. persicae*. Both aphid species are Aphididae, but belong to different subfamilies (*P. passerinii* is
128 the only member of the Phloeomyzinae while *M. persicae* is an Aphidinae), which diverged at 137 Ma
129 [27]. Compared to *P. passerinii*, *M. persicae* exhibit a quite different feeding strategy since it is a sap-
130 feeder, which host range does not include poplars, and preliminary establishment attempts confirmed
131 that it cannot settle and develop on poplars (data not shown). Firstly, considering both species allowed
132 to compare secretomes from two aphids with distinct feeding strategies, and to test whether the
133 atypical feeding strategy of *P. passerinii* results in an unusual saliva composition, particularly enriched
134 with potential effectors. Secondly, it allowed to compare poplar response during an interaction with a
135 specialist parasite, to poplar response during a non-host species interaction, i.e. an interaction that
136 would act as a positive control for defense reaction.

137 All individuals of *P. passerinii* used either for transcriptomic analyses of salivary glands or saliva collection
138 originated from the same monoclonal colony established from an apterous parthenogenetic female,
139 collected in 2013 in Brézé (France, 47°16’36’’ N 0°06’84’’ W, WGS-84). The colony was maintained in the
140 laboratory on potted stem cuttings of I-214, a *Populus x canadensis* Moench. genotype, under 20 ± 1 °C,
141 70 ± 10% relative humidity and 16/8 h light/dark cycles. Individuals of *M. persicae* originated from a
142 monoclonal colony established from an apterous parthenogenetic female collected in 1999 on a potato
143 plant in Loos-en-Gohelle (France, 50°27'44" N 2°46'45" E, WGS-84). The colony was maintained under
144 the same controlled conditions as *P. passerinii*, on turnips (Vilmorin).
145
146 Two *P. x canadensis* genotypes commonly planted in France, I-214 and Koster, were used for the
147 experiments. *Populus x canadensis* is a host species for *P. passerinii*. However, both genotypes differ in
148 their susceptibility to *P. passerinii*. I-214 is highly susceptible. The aphid shows high performance when
149 fed with this genotype, and can induce its reaction tissue within its cortical parenchyma. Conversely *P.*
150 *passerinii* cannot settle on Koster, and consequently induce a reaction tissue. This genotype is
151 consequently considered to be highly resistant [18]. Considering these two poplar genotypes allowed to
152 investigate interactions with *P. passerinii* leading either to an effector-triggered susceptibility, with the
153 susceptible I-214 genotype, or to resistance, with the resistant Koster genotype. *Populus x canadensis* is
154 not a host species for *M. persicae* and non-host species interactions between this aphid and both poplar
155 genotypes were consequently expected. Stem cuttings (ca. 25 cm long, 2 cm diameter) were provided by
156 the experimental nursery of Guéméné-Penfao (Office National des Forêts, France). They were collected
157 in the autumn of 2016, and kept at 2°C, in dry conditions until use. In January 2017, the stem-cuttings
158 were removed from storage and planted in 0.4 L pots, filled with a sterile sand-compost (50:50) mixture
159 (Klasmann substrate 4 no. 267). The cuttings were then transferred to a growth chamber (20 ± 1°C, 70 ±

160 10% relative humidity, 16/8 h light/dark photoperiod, 2.65 kLx, and watered three times a week). Leaves
161 were then used for protoplast production (see 2.3.3).
162 For *in planta* functional validation of the effects of salivary proteins, two transgenic lines of *Arabidopsis*
163 *thaliana* (L.) Heynh. were used. The transgenic line *pIAA2*::GUS [28] was used to assess the auxin
164 response, with its auxin-responsive promoter, while the cytokinin response was evaluated with
165 *pARR16*::GUS, with its cytokinin-responsive promoter [29]. Seeds were sterilized with chloral gas, sown
166 in Petri dishes on 0.8% (w/v) agar with 1% (w/v) sucrose-containing 0.5 Murashige and Skoog medium
167 (MS), stored for 2 days at 4°C, and grown on vertically oriented plates in growth chambers under a 16/8
168 h light/dark photoperiod at 18°C.
169
170 **2.2 Salivary transcriptome**
171
172 **2.2.1 Sample collection, RNA isolation and *de novo* transcriptome assembly**
173 About 500 adults of apterous parthenogenetic *P. passerinii* aphids, collected directly on their host-plant,
174 were dissected to collect pairs of salivary glands. Total RNA was extracted using the GeneJET RNA
175 Purification kit (Thermo Fischer Scientific), according to manufacturer's instructions. RNA was DNase
176 treated using RNase-Free DNase Set (Qiagen). RNA concentration was measured using the Qubit® RNA
177 Assay Kit (Life Technologies) and a Qubit® 2.0 Fluorometer (Invitrogen). Construction of cDNA-library and
178 sequencing were performed by Eurofins® Genomics using a MiSeq v3 Reagent Kit (600 Cycles PE,
179 Illumina, USA) and a MiSeq sequencer (Illumina), with 12.5 µg of total RNA. For the *de novo*
180 transcriptome assembly, 15,453,942 pair-ended reads were sequenced and assembled using Velvet
181 (v1.2.10; [30]) and Oases (v0.2.8; [31]) software tools (table S1). A multi-kmer approach was applied.
182 Separate assemblies with different kmer lengths were conducted and the individual assemblies were
183 merged to a final assembly. Kmer lengths of 69, 89, 109 and 129 were used. The separate assemblies

184 were merged following the filter1-CD-HIT-EST procedure proposed in Yang & Smith [32]. A completeness
185 assessment was performed using gVolante (v1.2.1; [33]) with the pipeline BUSCO v2/v3 and the
186 reference dataset Arthropoda (table S1). This Transcriptome Shotgun Assembly project was deposited at
187 DDBJ/EMBL/GenBank under the accession GHDF00000000. The version described in this paper is the first
188 version, GHDF01000000.
189

190 **2.2.2 Annotation, secreted proteins detection and identification**

191 To perform comparisons with *M. persicae* the transcriptome of this aphid was retrieved on NCBI
192 (http://www.ncbi.nlm.nih.gov/genbank/, accession numbers: DW010205 - DW015017, EC387039 -
193 EC390992, EE570018 - EE572264, EE260858 - EE265165, ES444641 - ES444705, ES217505 - ES226848,
194 and ES449829 - ES451794). Salivary transcriptomes were annotated using the pipeline described in figure
195 S1. Transcripts were first translated into amino acid sequences using Prodigal (v2.5; [34]). We then used
196 the SignalP 4.0 Server (v4.1) to predict the presence of signal peptides and cleavage sites in the amino
197 acid sequences [35]. To predict transmembrane domains, we submitted each amino acid sequence with
198 a signal peptide to the TMHMM Server (v. 2.0; [36]). Putative proteins with a signal peptide and no
199 transmembrane domain were considered to be potential secreted proteins. The sequences of complete
200 ORFs without signal peptide were analyzed again with SecretomeP (v2.0; [37]). To remove mitochondrial
201 proteins with a signal peptide, which are not secreted in the saliva, sequences were analyzed with
202 TargetP (v1.1; [38]). Likewise, to remove proteins of the endoplasmic reticulum with a signal peptide,
203 sequences were analyzed with PS-scan (Prosite pattern: PS00014), and with PredGPI [39] for
204 glycosylphosphatidylinositol-anchor signals.
205 The remaining proteins were first mapped against the non-redundant protein sequences (nr) using
206 Blastp (v2.3.0, NCBI, accessed on 03/30/2016), with an E-value cutoff at 1^{e-3}. Protein domains were
207 annotated with Blast2Go (v3.3; [40]), and InterProScan (v5.30-69; [41]). Whenever possible, protein

208 sequences were assigned to Gene ontology (GO) terms with an E-value cutoff at 1^{e-6}, enzyme codes (EC)
209 and KEGG pathways.
210 OrthoVenn (http://aegilops.wheat.ucdavis.edu/OrthoVenn; [42]) was used to identify orthologous
211 proteins within and between salivary transcriptomes of the two aphids. Intraspecific orthologous
212 proteins are first grouped into clusters, which are then compared between species. Each cluster was
213 annotated with the Uniprot database (http://www.uniprot.org; [43]) and the nr peptide sequence
214 database (NCBI, accessed on 03/30/2016).
215 To detect proteins orthologous to salivary effectors of aphids, protein sequences of known aphid
216 effectors, i.e. C002, ACE1, ACE2, ACYPI39568, ACYPI00346, MpC002, Mp1, Mp2, Mp42, Mp55, Me10,
217 Me23 [44, 45, 46], were compared to the salivary transcriptome of *P. passerinii* with Blastp (E-value ≤ 1^{e-}
218 ^{3}).
219
220 **2.3 Functional validation assays**
221
222 **2.3.1 Aphid saliva collection**
223 Aphids secrete two types of saliva within their host-plants, liquid and solid saliva [4]. The solid saliva is
224 secreted during probing. It hardens rapidly and forms a solid sheath encasing aphid stylets within the
225 host-plant, while the liquid saliva is secreted within cells and sieve tubes [4]. Both types of saliva contain
226 effectors [e.g. 4, 47], and were collected in our experiments. Because of the particular trophic substrates
227 of *M. persicae* and *P. passerinii* (i.e. sap and cortical tissues, respectively), a special protocol was used for
228 each species. The saliva of *P. passerinii* was collected after incubation of 30 to 40 individuals of 2nd and
229 3rd instars aphids on sachets of Parafilm© membranes containing an artificial diet [48]. The artificial diets
230 were constituted by a disc of 0.5% (w/v) agar completed with 150 µL of 15% (w/v) sucrose. The saliva of
231 *M. persicae* was collected after incubation of 30 to 40 individuals, of 3rd and 4th instars, on artificial diet

232 containing 120 µL of a 15% (w/v) sucrose as previously described by Cherqui & Tjallingii [48]. Aphids
233 were deposited in a feeding chamber during 24 h at 20°C, 60 ± 1% relative humidity and a 16/8 h
234 light/dark period with 2.65 kLx. Feeding chambers containing the artificial diets, incubated in the
235 absence of aphids, were used as control samples.
236 For *P. passerinii*, after 24 h aphid salivation, artificial diet discs were collected and transferred into 100
237 µL of TE buffer (10 mM Tris, 1 mM EDTA, pH 8). The salivary proteins were released from the artificial
238 diet according to Yang et al. [49], with slight modifications. The tubes containing artificial diet discs were
239 frozen in liquid nitrogen for 1 min, immediately thawed at 70°C for 3 min and then centrifuged at 11,000
240 x *g* for 20 sec. To discard the excess of agar, salivary extracts were centrifuged in Sartorius tubes with
241 filters of 0.22 µm. The supernatant containing salivary proteins of *P. passerinii* were collected, pooled
242 and then stored at -20°C. For *M. persicae,* after 24 h salivation, aphid saliva was collected according to
243 Harmel et al. [25]. The artificial diet is collected containing soluble saliva. The solid saliva was collected
244 during the rinsing of each lower Parafilm membrane with TE buffer containing 0.1% (w/v) of Tween 20
245 (TE/Tween). The extracts were centrifuged at 10,000 x *g* for 15 min. The salivary proteins in the pellet
246 were collected, pooled with the soluble saliva and then stored at -20°C.
247 The sample containing protein saliva extracts were concentrated using 2 mL Vivaspin© tube (Sartorius)
248 with 3kDa cut-off. The tubes were then centrifuged at 5,000 x *g* for 70 to 120 min according to sample
249 volumes, and proteins adhering to membranes were recovered by 100 µL of TE/Tween buffer. Control
250 samples were prepared with artificial diets from feeding chambers without aphids. The protein
251 quantification was performed by measuring absorbance at 280 nm with the NanoDrop© 1000
252 (ThermoScientific).
253
254 **2.3.2 Enzyme activities**

255 Several enzyme substrates were added to the previously described artificial diets with or without
256 agarose to detect enzymatic activities present in saliva excreted from the aphid. To visualize proteins in
257 the salivary sheaths, the lower Parafilm© membranes were stained by adding a drop of 0.01% (w/v)
258 Coomassie blue in 10% (v/v) glycerol for 2 h. Dihydroxyphenylalanine (DOPA), 0.1% (w/v) was added to
259 identify phenoloxidase activity (PO; catechol oxidase, EC 1.10.3.1). The enzymatic product, melanin,
260 should stain salivary sheaths and halos around the sheaths. To detect peroxidase (EC 1.11.1.7) activity,
261 artificial diets were immersed for some minutes in 0.1% (w/v) diaminobenzidine (DAB, Sigma) in 50 mM
262 Tris (pH 7.5) containing 0.1% (v/v) H_2O_2 (Sigma). The enzymatic product should induce reddish staining of
263 salivary sheaths and halos. For identification of pectinase activity, 0.1% (w/v) of pectin (Sigma) was
264 added to the medium. After exposure to aphids, the gel was transferred for 3 h into a Petri dish
265 containing 50 mM citrate-phosphate buffer, at pH 5.0 to detect pectin (methyl) esterase (PME, EC
266 3.1.1.11) and at pH 6.4 to detect polygalacturonase (PG, EC 3.1.1.15). The gel was then stained with a
267 solution of 0.01% (w/v) ruthenium red (Sigma) for 1 h, and then washed several times with distilled
268 water. At pH 6.4, red halos around the salivary sheaths indicate PME activity, while non-staining halos at
269 pH 5 in the pink pectin indicate PG activity. Finally, for proteinase activity (EC 3.4.99), 0.5% (w/v) of
270 gelatin (Sigma) was added to the medium. After exposure to aphids, the medium was incubated
271 overnight in a solution of 50 mM Tris (pH 8) containing 100 mM NaCl and 10 mM $CaCl_2$, then stained with
272 Coomassie blue. An absence of blue staining shows proteinase activity. All observations of proteins and
273 enzymatic activities were performed by light microscopy (Axioplan 2, Zeiss, Jena, Germany).
274

275 **2.3.3 Poplar protoplast preparations and treatments**

276 We wanted to assess early poplar gene responses to aphid saliva, as interactions between elicitors and
277 effectors of herbivores and plant receptors occur readily after the onset of probing or feeding [50]. Once
278 deposited on their plant material, adults and nymphs of *P. passerinii* can wait for several hours before

279 probing and delivering saliva into host tissues, inject probably a varying amount of saliva and presumably
280 affect a limited number of host cells [19, 20]. Therefore, we used protoplasts as plant material in order
281 to (i) have a sufficient amount of plant material exposed to treatments for the RT-qPCR experiments, (ii)
282 have an identical exposure duration and intensity to salivary extracts among biological replicates, and
283 (iii) avoid the effects of physical stimuli exerted by aphid stylets on plant cells. Mesophyll protoplasts of
284 the two poplar genotypes were obtained from young leaves as described in Wu et al. [51]. Leaves were
285 cut into 1–2 mm fine strips in 0.3 M sorbitol and 66.67 mM $CaCl_2$ (pH 5.6) and lysed in an enzyme
286 solution (0.6 M mannitol, 0.25% (w/v) cellulase Onozuka R-10, 0.05% (w/v) macerozyme R-10) in the
287 dark for 16 h with gentle shaking (30 rpm) at room temperature. Protoplasts were collected by filtering
288 the lysate suspension through a 70 µm cell strainer (Falcon®) and concentrated by spinning down at ≈
289 800 x *g* for 10 min at 4 °C. The pellet was washed twice with W5 buffer (154 mM NaCl, 125 mM $CaCl_2$, 5
290 mM KCl, 5 mM glucose, 0.03% (w/v) MES, pH 5.8) and then resuspended in 0.6 M mannitol to a final
291 concentration of 1×10^6 protoplasts per mL. Protoplasts (1.10^6) were incubated at 20°C with gentle
292 shaking (40 rpm) for 3 h with aphid salivary proteins or with protein extraction buffer (control). This
293 incubation duration allowed to observe early gene response to salivary effectors before cell walls start to
294 replenish [52]. RNA extraction was done just after the saliva or control treatment (see 2.3.4). Preliminary
295 experiments investigating expression of 5 poplar genes, and conducted with 1, 10, 20, 40 or 80 µg of
296 salivary proteins, indicated that the optimal response (i.e. the maximum fold change) was observed with
297 1 µg of salivary proteins of *P. passerinii* and 10 µg of salivary proteins of *M. persicae* (Fig. S2). Protoplast
298 viability, before and after treatment with aphid saliva, was assessed using 0.005% (w/v) fluorescein
299 diacetate (FDA). After 5 min of incubation protoplasts were observed under blue light epifluorescence,
300 and cell viability was estimated as the percentage of fluorescent cells. Most protoplasts were intact and
301 viable after enzymatic digestion with cellulase and macerozyme (98%), as well as after incubation with
302 salivary proteins (95%; Fig. S3).

303

304 **2.3.4 Quantitative RT-PCR**

305 After the aphid saliva treatments, protoplasts were centrifuged at ≈ 800 x *g* for 2 min. Total RNAs were
306 then immediately extracted with the RNeasy® Plant Kit Mini Kit (Qiagen). A DNase treatment with the
307 RNase-free DNase Set (Qiagen) was carried out for 15 min at 25°C. Total RNA concentration was
308 determined using a Nanodrop ND-1000 spectrophotometer. All RNA samples were rejected if they did
309 not reach a minimum concentration of 100 ng μL^{-1}, a 260 nm/280 nm ratio between 1.8 and 2.0. Poly(dT)
310 cDNA was prepared from 1 µg total RNA using the iScriptTMcDNA Synthesis Kit (Bio-Rad) and quantified
311 with a LightCycler 480 (Roche) and SYBR GREEN I Master (Roche), according to the manufacturer's
312 instructions. PCR was carried out in 384-well optical reaction plates heated for 10 min to 95°C to activate
313 hot start Taq DNA polymerase, followed by 40 cycles of denaturation for 60 sec at 95°C and
314 annealing/extension for 60 sec at 58°C. The distribution of the quantitative RT-PCR mix containing SYBR
315 Green I Master (Roche), cDNAs and primers was performed using the EVO150© (Tecan) pipetting robot in
316 a 384-well plate. The expression of 43 genes, belonging to eight different physiological processes or
317 metabolic pathways (i.e. auxin, cytokinins, jasmonates, ethylene, salicylic acid, phenolic compounds,
318 reactive oxygen species (ROS), cell-division cycle), was quantified with specific primer pairs designed by
319 Quant-Prime [53] based on the *Populus trichocharpa* sequence (v3.0) from Phytozome
320 (https://phytozome.jgi.doe.gov/pz/portal.html; Table S2). Expression levels were normalized to the
321 levels of *PtUBIQUITIN10* (*PtUBQ10*), commonly used as a reference gene in plants [e.g. 54]. All RT-qPCR
322 experiments were done with three independent biological replicates, with two technical replicates each.
323 One of the biological replicates of the *M. persicae* – Koster interaction was excluded from the analyses
324 because of technical issues during quantification. Relative gene expression was calculated according to
325 the $^{\Delta\Delta}$Ct method, with protoplasts incubated with protein extraction buffer as controls. Primers used for
326 gene expression analysis are listed in Table S2.

327

328 **2.3.5 Histochemical analysis of GUS activity**

329 Transgenic seedlings of *A. thaliana* (five-day-old and eight-day-old for *pIAA2*::GUS and *pARR16*::GUS,
330 respectively) were incubated with 2 mL of liquid MS containing 1 µg and 10 µg of aphid salivary proteins
331 (in TE/Tween buffer) of either *P. passerinii* or *M. persicae* for 3 h and 4 h for *pIAA2*::GUS and
332 *pARR16*::GUS, respectively. Positive controls were incubated with 20 µM of indole acetic acid (IAA)
333 (Sigma-Aldrich), and 20 µM of 6-benzylaminopurine (BAP) (Sigma-Aldrich). Negative controls were
334 incubated in liquid MS and corresponding volumes of TE/Tween buffer. Five seedlings were used for
335 each modality. Seedlings were then incubated in reaction buffer containing 0.1 M sodium phosphate
336 buffer (pH 7), 2 mM ferricyanide, 2 mM ferrocyanide, 0.1% (v/v) Triton X-100 and 1 mg ml^{-1} X-Gluc for 1
337 up to 24 h in dark at 37 °C. Afterwards, chlorophyll was removed by destaining in 70% ethanol and
338 seedlings were cleared as described by Malamy and Benfey [55]. GUS expression was monitored by
339 differential interference contrast microscopy.

340

341 **2.4 Data analysis**

342 All tests were carried out with the statistical software R 2.11.0 [56]. RT-qPCR results were expressed as
343 fold-changes in gene expression compared to the reference gene *PtUBQ10*. Fold-changes were log_2 -
344 transformed. Following this transformation, fold-changes varied between $-\infty$ and $+\infty$, with negative
345 values corresponding to gene underexpression, positive values to overexpression and zero, to no change
346 in gene expression. To visualize similarities and differences in fold-changes a heatmap was built, with
347 genes in columns and modalities in lines. The heatmap was built with a Z-score, i.e. log_2 – transformed
348 fold changes which were normalized and centered per column. Hierarchical clustering, using Pearson
349 correlation as similarity metric, was performed to visualize the proximity among genes in columns and
350 among modalities in lines. The uncertainty of hierarchical clustering of modalities was assessed with

351 approximately unbiased p-values calculated with a multiscale bootstrap resampling, with 10,000
352 bootstrap replications, using the function pvclust() [57]. T-tests were performed with $^{\Delta}$Ct values to detect
353 significant changes in expression for each saliva treatment vs. controls. An analysis of variance, followed
354 with a Tukey test when significant, was also performed to compare the effect of treatment modalities
355 (i.e. aphid species and host genotype combinations) on log_2-fold changes of each gene.
356
357 **3 Results**
358
359 **3.1 Annotation, secreted proteins detection and identification**
360 From 36,312 and 3,233 transcripts, 1,243 and 221 transcripts were predicted to encode for secreted
361 salivary proteins in *P. passerinii* and *M. persicae*, respectively. About half of them (604) were annotated
362 for *P. passerinii* and 190 for *M. persicae*. Using OrthoVenn, 121 and 58 protein clusters were identified
363 for *P. passerinii* and *M. persicae*, respectively. About 17% of these clusters were common between the
364 two aphids (Table S3).
365 Blast2GO determined that *P. passerinii* salivary gland encoded proteins were predominantly binding
366 proteins and enzymes (Fig. 1, table S4). The most common enzymes were peptidases (especially serine-
367 type and cysteine-type endopeptidases), kinases (especially phosphatidylinositol phosphate (PIP)
368 kinases) and hydrolases. Several enzymes involved in the degradation of carbohydrates (i.e. cellulase,
369 trehalase, β-glucuronidase, mannosidase and glucosylceramidase), and of phenolic compounds (i.e.
370 peroxidase and oxidoreductase) were also identified (Fig. 1, table S4). Among binding proteins,
371 dimerization protein, nucleic acids binding (especially DNA binding), nucleotide binding (especially ATP
372 binding) and cation-binding (mostly calcium ion-binding and zinc-binding proteins) were the most
373 commonly found (Fig. 1, table S4). Proteins related to hormone activity were also identified. Glucose
374 dehydrogenases were also detected with OrthoVenn (table S3). Among the 12 aphid salivary effectors

375 considered, five were identified in *P. passerinii*, with low E-values (< 7 e^{-71}): Mp10, ARMET, ACE 1, ACE2
376 and ACE3.
377
378 **3.2 Enzyme activities**
379 Staining with Coomassie blue confirmed the protein nature of the salivary sheath material (Fig. 2A) and
380 DOPA staining indicated a phenoloxidase activity in the sheaths (Fig. 2B). Black halos were also observed
381 around some sheaths (Fig. 2B). Likewise, peroxidase activity was found in salivary sheaths and halos
382 around sheaths (Fig. 2C). However, no pectinesterase, polygalacturonase and proteinase activity was
383 detected.
384
385 **3.3 Quantitative poplar gene expression**
386 An overview of poplar genes responses to aphid saliva is presented in figure 3. The hierarchical clustering
387 of modalities (left dendrogram) showed that all biological replicates of interactions with the salivary
388 proteins of *M. persicae* (i.e. non-host species interactions) were grouped within a significant cluster, in
389 which a majority of poplar genes were upregulated. Within this cluster, replicates were not arranged
390 according to poplar genotype. Biological replicates of the interaction between salivary proteins of *P.*
391 *passerinii* and Koster (i.e. the host species – resistant genotype) also clustered together, although the
392 cluster was significant for only two replicates. In this group, a majority of genes were weakly expressed
393 or upregulated. For biological replicates of the interaction between salivary proteins of *P. passerinii* and
394 I-214 (i.e. the host species - susceptible genotype), a majority were weakly expressed or downregulated.
395 Nonetheless, these replicates were not significantly clustered together. The hierarchical clustering of
396 genes (upper dendrogram) showed that there was no clustering of genes according to physiological
397 process or metabolic pathway.
398

399 For the auxin pathway, during non-host species interactions between salivary proteins of *M. persicae*
400 and both poplar genotypes biosynthetic genes were either not affected (*PtYUCCA*) or downregulated
401 (*PtNIT1*) while *PtGH3*, which is involved in auxin inactivaton via conjugation, was upregulated (Fig. 4).
402 *PtAPB1* (signaling) and *PtPIN1* (auxin efflux carrier) were also significantly upregulated, but only during
403 the interaction between *M. persicae* and I-214. No change was observed in the expression of the auxin
404 influx carrier *PtAUX1*. For *P. passerinii*, during the interaction with Koster these genes displayed an
405 expression profile quite similar to that observed during non-host species interactions with *M. persicae*,
406 except for *PtNIT1* whose expression was not affected. The expression of *PtGH3* was significantly
407 downregulated during the interaction between salivary proteins of *P. passerinii* and I-214, and *PtGH3*,
408 *PtAPB1* and *PtPIN1* were differentially expressed during the interaction with this susceptible genotype
409 compared to non-host species interactions with *M. persicae*, and compared to the interaction with the
410 resistant genotype for *PtAPB1* only (Fig. 4).
411 For the cytokinin pathway, during the non-host species interaction between salivary proteins of *M.*
412 *persicae* and I-214 *PtIPT* (biosynthesis), *PtAHK4* (perception) and *PtARR2* (signaling) were upregulated
413 while *PtLOG5* (metabolism) was significantly downregulated (Fig. 4). A similar expression profile was
414 observed during the non-host species interaction with Koster, but only *PtAHK4* and *PtLOG5* were
415 significantly affected. These genes were not significantly affected during the interaction between salivary
416 proteins of *P. passerinii* and Koster. In contrast, *PtARR2* was strongly repressed during the *P. passerinii* –
417 I-214 interaction, and *PtAHK4* and *PtARR2* were differentially expressed during this interaction compared
418 to the other ones (Fig. 4).
419 Regarding biotic stress signaling (i.e. jasmonates, salicylic acid, ethylene and ROS), non-host species
420 interactions were characterized by a marked upregulation of a majority of genes, which was more
421 frequently significant for the interaction with I-214 than for the interaction with Koster (Fig. 5). Few
422 genes in jasmonate ethylene and ROS pathways were not affected by salivary extracts of *M. persicae* (i.e.

423 *PtAOS*, *PtJAZ1*, *PtEIN2*, *PtETO1*, *PtCAT* and *PtSOD*), and, in the salicylic acid pathway, *PtPR5* was
424 significantly downregulated. For interactions with salivary proteins of *P. passerinii*, all genes were weakly
425 downregulated during the interaction with the susceptible genotype. In contrast, during the interaction
426 with the resistant genotype most genes were either not affected or exhibited profiles as during non-host
427 species interactions with *M. persicae*, with weak upregulations. Nonetheless, for these modalities, no
428 gene expression significantly differed from the controls (Fig. 5). In most cases, gene expressions during
429 the interaction with the susceptible genotype were significantly lower than during non-host species
430 interactions with I-214, and, in fewer cases, lower than during non-host species interactions with Koster.
431 For interactions with *P. passerinii*, only *PtCOI1* and *PtEIN3* genes were differentially expressed during
432 interactions with either the susceptible or the resistant genotype. Conversely, since gene expressions
433 during interactions with the resistant genotype were weakly upregulated, they generally did not differ
434 from those observed during non-host species interactions with Koster, and differed from non-host
435 species interactions with I-214 for only several genes (i.e. *PtCOI1*, *PtEDS1*, *PtNPR1*, *PtNDR1*, *PtEIN3*,
436 *PtADMS1*). Nonetheless, *PtPR5* and *PtSOD* were clearly differentially expressed between host and non-
437 host interactions with Koster.
438 For genes involved in the phenolic compounds pathway (Fig. 5), non-host species interactions, especially
439 with I-214, led to an upregulation of all the considered genes. All genes were weakly, but not
440 significantly, downregulated or upregulated during interactions between the saliva of *P. passerinii* and
441 either the susceptible genotype or the resistant genotype, respectively. For I-214, gene expression was
442 always significantly lower during the interaction with the saliva of *P. passerinii* compared to the
443 interaction with the saliva of *M. persicae*. For *PtF5H*, expression was also significantly lower during the *P.*
444 *passerinii* – I-214 interaction compared to other interactions.
445 Finally, regarding genes involved in cell-division cycle, *PtCDK5*, *PtPCNA*, *PtCDK20 and PtE2F* were
446 significantly upregulated during non-host species interactions with *M. persicae*, while *PtCAK1* was

447 significantly downregulated (Fig. 6). *PtCYCD5* and *PtACO1* were also upregulated but only during non-
448 host species interactions with I-214. Likewise, *PtCDK5* and *PtCDK20* were also significantly upregulated
449 during the *P. passerinii* - Koster interaction, as well as *PtCAK1*. Expression of *PtMCM2* and *PtRBR* was not
450 affected by salivary extracts. *PtCDK20* was differentially expressed during the *P. passerinii* - I-214
451 interaction compared to other ones. Likewise, during the *P. passerinii* - Koster interaction the expression
452 of *PtCTR1* was much lower compared to non-host species ones and expression of *PtE3UL*, *PtE2F* and
453 *PtACO1* were lower compared to expression during non-host species interactions with I-214. For *PtCAK1*,
454 the expression was higher during the *P. passerinii* - Koster interaction than during non-host species ones.
455

456 **3.4 Histochemical analysis of GUS activity**

457 Salivary extracts of *P. passerinii* increased *pIAA2*::GUS signals (Fig. 7E, 7F, 7I, 7J), which were similar to
458 those caused by an exogenous application of auxin (Fig. 7A and 7B). Incubation with salivary proteins of
459 *M. persicae* resulted in faint colorations (Fig. 7G, 7H, 7K, 7L), similar to those of negative controls (Fig. 7C
460 and 7D).
461 Positive controls of *pARR16*::GUS were characterized by a strong staining in the middle part of root
462 central cylinder (Fig. 8A and 8B), which was weak in negative controls as well as with *M. persicae* salivary
463 proteins (Fig. 8G, 8H, 8K, and 8L). No coloration was visible in the roots of seedlings incubated with
464 salivary proteins of *P. passerinii* (Fig. 8E, 8F, 8I and 8J).
465

466 **4 Discussion**

467

468 Successful plant colonization by parasites generally requires the circumvention or inactivation of host
469 defenses, and sometimes a finely tuned reprogramming of host metabolism. As a consequence, the
470 lifestyle and feeding strategy of parasites should have both quantitative and qualitative outcomes on

471 their secretome [e.g. 11, 58]. In line with this, comparisons among salivary proteins of aphid species also
472 indicated that aphids with different host species and / or feeding strategies exhibited very different
473 salivary protein profiles [59, 60]. Our results tend to support this assertion since the predicted salivary
474 gland proteins of *P. passerinii* and *M. persicae* shared few similarities, and poplar gene expression
475 profiles markedly differed when protoplasts were exposed to salivary proteins of these two aphid
476 species. The salivary transcriptome of *P. passerinii* also hold specific and abundant PIP kinases
477 sequences, which have never been reported from any other aphid saliva. Nonetheless, several protein
478 functions predicted in our study (e.g. calcium-binding, DNA-binding, ATP-binding, GTP-binding proteins,
479 glucose dehydrogenases, oxidoreductases, trehalases and phosphatases) have also been identified in the
480 saliva of different sap-feeding aphid species [22, 59, 61, 62], and in secretions of other plant parasites [3,
481 63]. Interestingly, calcium-binding proteins are supposedly key components of the saliva of sap-feeding
482 aphids, preventing the plugging of sieve tubes [4]. Since *P. passerinii* does not feed on sap [19], it
483 suggests that these proteins also play other crucial roles during aphid-plant interactions. In addition to
484 their different feeding strategies, the two aphid species are also phylogenetically distant [27], which
485 should further increase the dissimilarity of their secretomes. It should be noted also that the
486 transcriptomes of *P. passerinii* and *M. persicae* have been obtained with a different sequencing and
487 assembly methods [64]. This probably explains the difference in transcripts amounts gathered for both
488 aphids and several encoded proteins in salivary glands of *M. persicae* might be missing in its
489 transcriptome, leading to an apparently low similarity between secretomes. Likewise, the lack of
490 biological replicates for both transcriptomes might have also led to an underestimation of the similarity
491 between secretomes.
492
493 Several encoded proteins detected in the salivary glands of *P. passerinii* may interfere with host defenses
494 *via* direct interactions with secondary metabolites or defense proteins. The interaction between *P.*

495 *passerinii* and susceptible poplar genotypes is characterized by transient accumulation of phenolic
496 compounds, which fade away during later stages of the interaction [20]. Salivary effectors might
497 contribute to the degradation of these secondary metabolites as numerous oxidoreductase sequences
498 were identified in the salivary gland transcriptome of *P. passerinii*. Moreover, *in situ* biochemical assays
499 confirmed the presence of active peroxidases and phenoloxidases in both solid and soluble saliva
500 fractions of *P. passerinii*. The predicted glucose dehydrogenases may also help *P. passerinii* to detoxify
501 defensive compounds of the host-plant [11, 60]. Likewise, plant defense proteins might be inactivated by
502 the numerous protein-binding proteins and proteases predicted among the salivary gland encoded
503 proteins of *P. passerinii*. Parasites frequently secrete similar effectors to degrade or modulate the plant
504 enzymes activities [3]. Nonetheless, no protease activity was observed during *in situ* bioassays. Gelatin
505 was probably not the adequate substrate to detect the protease activity of *P. passerinii*. Additional *in situ*
506 assays could be conducted to detect, in *P. passerinii* saliva, the activity of the proteases and possibly
507 other enzymes like cellulases. A proteomic analysis of salivary extracts should also confirm and
508 complement the predictions of our transcriptomic approach [65, 66].
509 Several salivary gland encoded proteins may also affect host defense *via* a disruption of biotic stress
510 signaling. PIP kinases catalyze phosphorylation of phosphatidyl-inositol into phosphatidylinositol-4-5-
511 biphosphate (PIP_2). The hydrolysis of PIP_2 produces secondary messengers like inositol-1-4-5-
512 triphosphate (IP_3) and diacylglycerol (DAG). This latter can in turn be hydrolyzed into phosphatidic acid
513 (PA) considered an important signaling molecule in plants, triggered in response to various biotic and
514 abiotic stresses [67]. PIP_2 and IP_3 might also affect cellular oscillations of cytosolic Ca^{2+} and are involved in
515 multiple processes including cell cycle and phytohormone regulation [68]. Other proteins, also frequently
516 detected in parasites, including aphids, may also interfere with secondary messengers like calcium-
517 binding, ATP-binding, and GTP-binding proteins or with hormone signaling like hormone-binding proteins

518 [3, 5, 6, 59]. Similarly, it has been hypothesized that trehalase may interfere with trehalose-based
519 defense responses in *A. thaliana* [61].
520 Finally, several salivary gland encoded proteins could also contribute to the manipulation of host-plant
521 metabolism. For instance, nucleic acid-binding proteins could affect gene expression, while protein-
522 binding and hormone-binding proteins could modulate metabolic and phytohormonal pathways [3, 59].
523 In addition, serine proteases, acid phosphatases, cellulases, lipases and metalloproteases have also been
524 predicted or detected in the secretions of different gall-inducing organisms, and supposedly contribute
525 to gall induction and / or maintenance [63, 69].
526
527 Both the *in vivo* approach with protoplasts and the heterologous *in planta* assay with *A. thaliana*
528 confirmed that salivary proteins of *P. passerinii* impact plant gene transcription, in a specific manner.
529 Gene expression profiles markedly differed, especially in terms of intensity, between non-host species
530 interactions with *M. persicae* and host species interactions with *P. passerinii*. Non-host species
531 interactions led to an upregulation of most genes involved in jasmonate, ethylene and salicylic acid
532 pathways, which are typically activated following aphid feeding, together or separately, depending on
533 the aphid – plant interaction system considered [70, 71, 72]. As a consequence, genes related to
534 secondary metabolism, i.e. *PtF3'5'H, PtANT* and *PtF5H*, were also upregulated during these interactions.
535 Conversely, the expression of genes related to biotic stress signaling and defense was either unaffected
536 or slightly downregulated or upregulated during interactions with a susceptible and a resistant genotype
537 of the host species, respectively. This suggests that salivary effectors of *P. passerinii* manage to inactivate
538 or bypass the biotic stress signaling in their host plant, as frequently observed in plant-parasites
539 interactions [1, 3]. Non-host species interactions with the two poplar genotypes led to similar gene
540 expression profiles while, for interactions with *P. passerinii*, the expression of several genes differed
541 according to host genotype. Among them, the expression of several genes involved in biotic stress

542 signaling (*PtCOI1*, *PtEIN3*), and defense (*PtF5H*), was significantly higher during the interaction with the
543 resistant genotype than during the interaction with the susceptible one. The overall trend of lack of
544 response or downregulation of genes involved in defense or biotic signaling observed during the
545 interaction between salivary extracts of *P. passerinii* and the susceptible host genotype is congruent with
546 gene expression profiles observed during effector-triggered susceptibility in other plant-parasite systems
547 [73, 74].
548 Although different from the interaction with a susceptible genotype, the interaction between the
549 resistant genotype and *P. passerinii* did not lead to marked upregulations of genes related to biotic stress
550 signaling or defense. Gene expression profiles of poplar protoplasts during the interaction between *P.*
551 *passerinii* and the resistant poplar genotype shared many similarities with those observed during non-
552 host species interactions with *M. persicae*. Both types of interactions were characterized by an overall
553 upregulation of host genes, which was generally more important during non-host species interactions
554 than during host species interaction with the resistant host genotype, for which only few significant
555 upregulations were observed. Interestingly, two of the three genes that were differentially expressed
556 during non-host and incompatible interactions on the same poplar genotype (i.e. *PtPR5* and *PtSOD* –
557 with a similar trend for *PtCAT*) were related to biotic stress signaling, and were slightly upregulated
558 during the interaction with the resistant genotype while they were significantly downregulated during
559 non-host species interactions. Effector-triggered immunity is generally a strong defense response,
560 associated with extensive and rapid transcriptional reprogramming [10, 74, 75]. This was not detected
561 during interactions between *P. passerinii* and the resistant host genotype. Nonetheless the reprograming
562 can take place within few hours [75], and the incubation duration might have been too short to detect an
563 extensive reprogramming. Slightly longer incubation durations might solve this issue.
564

565 To knock-down or divert stress signaling parasites may also reconfigure auxin and cytokinin signaling
566 pathways [1, 6, 76]. Both RT-qPCR experiments and histochemical assays confirmed that *P. passerinii* can
567 actively manipulate both auxin and cytokinin pathways during an interaction with a susceptible host
568 genotype. Salivary extracts of *P. passerinii* did not affect either auxin biosynthesis or auxin transporter
569 genes such as *PtPIN1* and *PtAUX1*, but significantly downregulated *PtGH3*, which is involved in the
570 homeostasis of active auxin forms [77]. This could lead to intracellular accumulation of active auxin
571 forms, which is supported by the activation of the auxin-responsive promoter *IAA2* during *in planta*
572 assays with transgenic seedlings of *A. thaliana*. Auxin accumulation could in turn interfere with salicylic
573 acid signaling and defense responses [77], which would be congruent with the overall absence of
574 response of genes related to the salicylic acid pathway (Fig. 9). As genes related to cytokinin biosynthesis
575 (*PtIPT*) and activation (*PtLOG5*) were not affected by salivary proteins of *P. passerinii*, the
576 downregulation of cytokinin perception and signaling genes (*PtAHK4* and *PtARR2* during the assays with
577 protoplasts and *ARR16* during the assay with *A. thaliana*) could correspond to an auxin accumulation-
578 induced regulation loop [78, 79]. This downregulation of *PtAHK4* and *PtARR2* could also interfere with
579 stress signaling by preventing both accumulation of jasmonate and activation of *PtPR1* [80] (Fig. 9).
580
581 The intracellular accumulation of active auxin forms could also contribute to the targeted cell
582 hypertrophy and multiplication commonly observed in the reaction tissues induced by *P. passerinii* in
583 susceptible poplar genotypes [20] (Fig. 9). Auxin accumulation, as a result of a reduction in both *GH3*
584 activity and auxin transport, is also probably involved in the initiation and development of root galls by
585 cyst and root-knot nematodes [81]. However, exposure of protoplasts of the susceptible genotype to the
586 salivary extracts of *P. passerinii* did not affect expression of genes involved in the cell-division cycle, or
587 weakly downregulated them. Only one gene involved in cell-division cycle (i.e. *PtCDK20*) was
588 differentially expressed during interactions with either a susceptible or a resistant host genotype.

589 Additional experiments considering genes coding for cell wall remodeling enzymes, activated early
590 during root-knot nematode-induced giant cell differentiation, or for cytoskeleton should provide further
591 insight into the mechanisms associated with the differentiation of hypertrophied cells in this system [73].
592
593 In conclusion, our transcriptomic analysis of the saliva of *P. passerinii* and *M. persicae* showed that *P.*
594 *passerinii* probably secretes a highly peculiar saliva, filled with potential effectors that may interfere with
595 several plant secondary messengers and signaling pathways. Our *in vivo* approach with protoplasts and
596 *in planta* approach with a heterologous *A. thaliana*-system confirmed the ability of salivary extracts of *P.*
597 *passerinii* to interfere with host response during interactions with a susceptible host genotype. As
598 expected auxin and cytokinin pathways were affected, probably to impair biotic stress signaling but also
599 to reconfigure host metabolism and anatomy. Although the saliva of *P. passerinii* and *M. persicae* were
600 very different, interactions with non-host species and with a resistant genotype of a host species led to
601 quite similar host responses, with a different intensity however, and few differences in biotic stress
602 signaling and cytokinin metabolism. Additional modalities including different populations of *P. passerinii*,
603 different poplar genotypes with intermediate resistance levels [18], and additional host metabolic
604 pathways could be considered in future experiments. For instance, investigating how genes coding for
605 NB-LRR proteins, involved in the induction of effector-triggered immunity following the recognition of
606 parasite effectors [10, 82], respond to salivary extracts of *P. passerinii* should give further insights into
607 the molecular processes underpinning failed and successful host infestation by *P. passerinii*. Similarly,
608 investigating the response of genes coding for early nodulin-like proteins, recently characterized in the
609 genome of *P. trichocarpa* [83], could help to unravel the molecular mechanisms underpinning host
610 manipulation, since these genes are targeted by several gall-inducing organisms [84, 85].
611
612

Funding

This work was supported by the Région Centre-Val de Loire Project no. 2014 00094521 (InsectEffect) coordinated by D. Giron.

Acknowledgements

We thank Léa Fléchon for her assistance with transcriptome analyses. We are also grateful to the reviewers for their valuable comments.

References

[1] S.A. Hogenhout, R.A. Van der Hoorn, R. Terauchi, S. Kamoun, Emerging concepts in effector biology of plant-associated organisms. Mol. Plant-Microbe Int., 22 (2009), 115-122.

[2] S.A. Hogenhout, J.I. Bos, Effector proteins that modulate plant–insect interactions. Curr. Opin. Plant Biol., 14 (2011), 422-428.

[3] J. Win, A. Chaparro-Garcia, K. Belhaj, D.G.O. Saunders, K. Yoshida, S. Dong, S. Schornack, C. Zipfel, S.A. Hogenhout, S. Kamoun, Effector biology of plant-associated organisms: concepts and perspectives. Cold Spring Harb. Symp. Quant. Biol. 77 (2012), 235-247.

[4] T. Will, W.F. Tjallingii, A. Thönnessen, A.J. van Bel. Molecular sabotage of plant defense by aphid saliva. Proc. Nat. Acad. Sci., 104 (2007), 10536-10541.

[5] A. Guiguet, G. Dubreuil, M.O. Harris, H. Appel, J.C. Schultz, M.H. Pereira, D. Giron, Shared weapons of blood- and plant-feeding insects: surprising commonalities for manipulating hosts. J. Ins. Physiol., 84 (2016), 4-21.

[6] D. Giron, E. Huguet, G.N. Stone, M. Body, Insect-induced effects on plants and possible effectors used by galling and leaf-mining insects to manipulate their host-plant. J. Ins. Physiol., 84 (2016), 70-89.

636 [7] L.Q. Chen, SWEET sugar transporters for phloem transport and pathogen nutrition. New Phytol., 201
637 (2014), 1150-1155.
638 [8] J. Sandström, A. Telang, N.A. Moran, Nutritional enhancement of host plants by aphids - a
639 comparison of three aphid species on grasses. J. Ins. Physiol., 46 (2000), 33-40.
640 [9] M.G. Mitchum, R.S. Hussey, T.J. Baum, X. Wang, A.A. Elling, M. Wubben, E.L. Davis, Nematode
641 effector proteins: an emerging paradigm of parasitism. New Phytol., 199 (2013), 879-894.
642 [10] P.N. Dodds, J.P. Rathjen, Plant immunity: towards an integrated view of plant–pathogen
643 interactions. Nat. Rev. Genet., 11 (2010), 539.
644 [11] L. Lo Presti, D. Lanver, G. Schweizer, S. Tanaka, L. Liang, M. Tollot, A. Zuccaro, S. Reissmann, R.
645 Kahmann, Fungal effectors and plant susceptibility. Ann. Rev. Plant Biol., 66 (2015), 513-545.
646 [12] M. Franceschetti, A. Maqbool, M.J. Jiménez-Dalmaroni, H.G. Pennington, S. Kamoun, M.J. Banfield,
647 Effectors of filamentous plant pathogens: commonalities amid diversity. Microbiol. Mol. Biol. Rev., 81
648 (2017), e00066-16.
649 [13] I. Kaloshian, L.L. Walling, Hemipteran and dipteran pests: effectors and plant host immune
650 regulators. J. Integr. Plant Biol., 58 (2016), 350-361.
651 [14] S. Basu, S. Varsani, J. Louis, Altering plant defenses: herbivore-associated molecular patterns and
652 effector arsenal of chewing herbivores. Mol. Plant-Microbe Int., 31(2017), 13-21.
653 [15] J.J. Stuart, M.S. Chen, R. Shukle, M.O. Harris, Gall midges (Hessian flies) as plant pathogens. Ann.
654 Rev. Phytopathol., 50 (2012), 339-357.
655 [16] J. Stuart Insect effectors and gene-for-gene interactions with host plants. Curr. Opin. Ins. Sci., 9
656 (2015), 56-61.
657 [17] D. Giron, G. Dubreuil, A. Bennett, F. Dedeine, M. Dicke, L.A. Dyer, M. Erb, M.O. Harris, E. Huguet, I.
658 Kaloshian, A. Kawakita, C. Lopez-Vaamonde, T.M. Palmer, T. Petanidou, M. Poulsen, A. Sallé, J.-C. Simon,

659 J. Terblanche, D. Thiery, N.K. Whiteman, H.A. Woods, S. Pincebourde (2018). Promises and challenges in
660 insect–plant interactions. Entomol. Exp. Appl., 166 (2017), 319-343.
661 [18] A. Sallé, S. Pointeau, S. Bankhead-Dronnet, C. Bastien, F. Lieutier, Unraveling the tripartite
662 interactions among the woolly poplar aphid, its host tree, and their environment: a lead to improve the
663 management of a major tree plantation pest? Ann. For. Sci., 74 (2017), 79.
664 [19] S. Pointeau, A. Ameline, F. Laurans, A. Sallé, Y. Rahbé, S. Bankhead-Dronnet, F. Lieutier, Exceptional
665 plant penetration and feeding upon cortical parenchyma cells by the woolly poplar aphid. J. Ins. Physiol.,
666 58 (2012), 857–866.
667 [20] F. Dardeau, E. Deprost, F. Laurans, V. Lainé, F. Lieutier, A. Sallé, Resistant poplar genotypes inhibit
668 pseudogall formation by the wooly poplar aphid, *Phloeomyzus passerinii* Sign., Trees, 28 (2014), 1007-
669 1019.
670 [21] A. Sallé, R. Jerger, C. Vincent-Barbaroux, O. Baubet, D. Dahuron, S. Bourgerie, F. Lieutier, Tree-killing
671 aphid dramatically reduces bark contents in carbohydrates and nitrogen compounds. For. Ecol. Manage.,
672 407 (2018), 23-30.
673 [22] F. Dardeau, M. Body, A. Berthier, F. Miard, J. P. Christidès, M. Feinard-Duranceau, F. Brignolas, D.
674 Giron, F. Lieutier, A. Sallé, Effects of fertilisation on amino acid mobilisation by a plant-manipulating
675 insect. Ecol. Entomol., 40 (2015), 814-822.
676 [23] F. Dardeau, S. Pointeau, A. Ameline, F. Laurans, A. Cherqui, F. Lieutier, A. Sallé, Host manipulation by
677 a herbivore optimizes its feeding behaviour. Anim. Behav., 95 (2014), 49-56.
678 [24] J.F. Tooker, A.M. Helms, Phytohormone dynamics associated with gall insects, and their potential
679 role in the evolution of the gall-inducing habit. J. Chem. Ecol., 40 (2014), 742–753.
680 [25] N. Harmel, E. Létocart, A. Cherqui, P. Giordanengo, G. Mazzucchelli, F. Guillonneau, E. De Pauw, E.
681 Haubruge, F. Francis, Identification of aphid salivary proteins: a proteomic investigation of *Myzus*
682 *persicae*. Ins. Mol. Biol., 17 (2008), 165–174.

683 [26] M. De Vos, G. Jander, *Myzus persicae* (green peach aphid) salivary components induce defence
684 responses in *Arabidopsis thaliana*. Plant Cell Environ., 32 (2009), 1548–1560.
685 [27] Z. Ren, A.J. Harris, R.B. Dikow, E. Ma, Y. Zhong, J. Wen, Another look at the phylogenetic
686 relationships and intercontinental biogeography of eastern Asian–North American Rhus gall aphids
687 (Hemiptera: Aphididae: Eriosomatinae): Evidence from mitogenome sequences via genome skimming.
688 Mol. Phylogenet. Evol., 117 (2017), 102-110.
689 [28] A. Bishopp, S. El-Showk, D. Weijers, B. Scheres, J. Friml, E. Benková, A. Pekka Mähönen, Y. Helariutta,
690 A mutually inhibitory interaction between auxin and cytokinin specifies vascular pattern in roots. Curr.
691 Biol., 21 (2011), 917-926.
692 [29] T. Kiba, H. Yamada, T. Mizuno, Characterization of the ARR15 and ARR16 response regulators with
693 special reference to the cytokinin signaling pathway mediated by the AHK4 histidine kinase in roots of
694 *Arabidopsis thaliana*. Plant Cell Physiol., 43 (2002), 1059-1066.
695 [30] D. Zerbino, E. Birney, Velvet: algorithms for de novo short read assembly using de Bruijn graphs.
696 Gen. Res., (2008), gr-074492.
697 [31] M.H. Schulz, D.R. Zerbino, M. Vingron, E. Birney, Oases: robust *de novo* RNA-seq assembly across the
698 dynamic range of expression levels. Bioinformatics, 28 (2012), 1086-1092.
699 [32] Y. Yang, S.A. Smith, Optimizing *de novo* assembly of short-read RNA-seq data for phylogenomics.
700 BMC Genomics, 14 (2013), 328.
701 [33] O. Nishimura, Y. Hara, S. Kuraku S. gVolante for standardizing completeness assessment of genome
702 and transcriptome assemblies. Bioinformatics, 33 (2017), 3635-3637.
703 [34] D. Hyatt, G.L. Chen, P.F. LoCascio, M.L. Land, F.W. Larimer, L.J. Hauser, Prodigal: prokaryotic gene
704 recognition and translation initiation site identification. BMC Bioinformat., 11 (2010), 119.
705 [35] T.N. Petersen, S. Brunak, G. von Heijne, H. Nielsen, SignalP 4.0: discriminating signal peptides from
706 transmembrane regions, Nat. Methods, 8 (2011), 785.

707 [36] R. Ji, H. Yu, Q. Fu, H. Chen, W. Ye, S. Li, Y. Lou, Comparative transcriptome analysis of salivary glands
708 of two populations of rice brown planthopper, *Nilaparvata lugens*, that differ in virulence. PloS One, 8
709 (2013), e79612.
710 [37] J.D. Bendtsen, L.J. Jensen, N. Blom, G. von Heijne, S. Brunak, Feature-based prediction of non-
711 classical and leaderless protein secretion. Prot. Eng. Des. Sel., 17 (2004), 349-356.
712 [38] O. Emanuelsson, H. Nielsen, S. Brunak, G. von Heijne, Predicting subcellular localization of proteins
713 based on their N-terminal amino acid sequence. J. Mol. Biol., 300 (2000), 1005-1016.
714 [39] A. Pierleoni, P.L. Martelli, R. Casadio, PredGPI: a GPI-anchor predictor. BMC Bioinformat., 9 (2008),
715 392.
716 [40] A. Conesa, S. Götz, J.M. García-Gómez, J. Terol, M. Talón, M. Robles, Blast2GO: a universal tool for
717 annotation, visualization and analysis in functional genomics research. Bioinformat., 21 (2005), 3674–
718 3676.
719 [41] P. Jones, D. Binns, H.Y. Chang, M. Fraser, W. Li, C. McAnulla, H. McWilliam, J. Maslen, A. Mitchell, G.
720 Nuka, S. Pesseat, A.F. Quinn, A. Sangrador-Vegas, M. Scheremetjew, S.-Y. Yong, R. Lopez, S. Hunter,
721 InterProScan 5: genome-scale protein function classification. Bioinformat., 30 (2014), 1236-1240.
722 [42] Y. Wang, D. Coleman-Derr, G. Chen, Y.Q. Gu. OrthoVenn: a web server for genome wide comparison
723 and annotation of orthologous clusters across multiple species. Nucleic Acids Res., 43 (2015), W78-W84.
724 [43] S. Pundir, M.J. Martin, C. O'Donovan, Uniprot protein knowledgebase, in: C. Wu, C. Arighi, K. Ross
725 (Eds). Protein Bioinformatics. Methods in Molecular Biology, vol 1558. Humana Press, New York, 2017,
726 41-55.
727 [44] K. Guo, W. Wang, L. Luo, J. Chen, Y. Guo, F. Cui, Characterization of an aphid-specific, cysteine-rich
728 protein enriched in salivary glands. Biophys. Chem., 189 (2014), 25–32.
729 [45] M. Jaouannet, P.A. Rodriguez, P. Thorpe, C.J.G. Lenoir, R. MacLeod, C. Escudero-Martinez, J.I.B. Bos,
730 Plant immunity in plant–aphid interactions. Front. Plant Sci., 5 (2014), 663.

731 [46] Y. Pan, J. Zhu, L. Luo, L. Kang, F. Cui, High expression of a unique aphid protein in the salivary glands
732 of *Acyrthosiphon pisum*. Physiol. Mol. Plant Pathol., 92 (2015), 175–180.
733 [47] D.A. Elzinga, G. Jander, The role of protein effectors in plant–aphid interactions. Curr. Opin. Plant
734 Biol., 16 (2013), 451-456.
735 [48] A. Cherqui, W.F. Tjallingii, W.F. Salivary proteins of aphids, a pilot study on identification, separation
736 and immunolocalisation. J. Ins. Physiol., 46 (2000), 1177–1186.
737 [49] J.L. Yang, R. Yang, A.C. Cheng, R.Y. Jia, M.S. Wang, S.H. Zhang, Five-minute purification of PCR
738 products by new-freeze-squeeze method. J. Food Agric. Environ., 8 (2010), 32–33.
739 [50] M.E. Maffei, A. Mithöfer, W. Boland, Insects feeding on plants: rapid signals and responses
740 preceding the induction of phytochemical release. Phytochemistry, 68 (2007), 2946-2959.
741 [51] F.H. Wu, S.C. Shen, L.Y. Lee, S.H. Lee, M.T. Chan, C.S. Lin, Tape-*Arabidopsis* Sandwich-a simpler
742 *Arabidopsis* protoplast isolation method. Plant Meth., 5 (2009), 16.
743 [52] J. Guo, J.L. Morrell-Falvey, J.L. Labbé, W. Muchero, U.C. Kalluri, G.A. Tuskan, J.G. Chen, Highly
744 efficient isolation of Populus mesophyll protoplasts and its application in transient expression assays.
745 PloS One, 7 (2012), e44908.
746 [53] S. Arvidsson, M. Kwasniewski, D.M. Riaño-Pachón, B. Mueller-Roeber, QuantPrime--a flexible tool
747 for reliable high-throughput primer design for quantitative PCR. BMC Bioinformat., 9 (2008), 465.
748 [54] Z. Tong, Z. Gao, F. Wang, J. Zhou, Z. Zhang, Selection of reliable reference genes for gene expression
749 studies in peach using real-time PCR. BMC Mol. Biol., 10 (2009), 71.
750 [55] J.E. Malamy, P.N. Benfey, Organization and cell differentiation in lateral roots of *Arabidopsis*
751 *thaliana*. Development, 124 (1997), 33-44.
752 [56] R Core Team (2013). R: A language and environment for statistical computing. R Foundation for
753 Statistical Computing, Vienna, Austria. URL http://www.R-project.org/.

754 [57] R. Suzuki, H. Shimodaira, Pvclust: an R package for assessing the uncertainty in hierarchical
755 clustering. Bioinformatics, 22 (2006), 1540-1542.
756 [58] Y. Cuesta-Astroz, F.S. de Oliveira, L.A. Nahum, G. Oliveira, Helminth secretomes reflect different
757 lifestyles and parasitized hosts. Int. J. Parasitol., 47 (2017), 529-544.
758 [59] S. Vandermoten, N. Harmel, G. Mazzucchelli, E. De Pauw, E. Haubruge, F. Francis. Comparative
759 analyses of salivary proteins from three aphid species. Ins. Mol. Biol., 23 (2014), 67-77.
760 [60] W.R. Cooper, J.W. Dillwith, G.J. Puterka, Comparisons of salivary proteins from five aphid
761 (Hemiptera: Aphididae) species. Environ. Entomol., 40 (2011), 151-156.
762 [61] S.J. Nicholson, S.D. Hartson, G.J. Puterka, Proteomic analysis of secreted saliva from Russian Wheat
763 Aphid (*Diuraphis noxia* Kurd.) biotypes that differ in virulence to wheat. J. Proteomics, 75 (2012), 2252–
764 2268.
765 [62] D.A. Elzinga, G. Jander, The role of protein effectors in plant–aphid interactions. Curr. Opin. Plant
766 Biol., 16 (2013), 451-456.
767 [63] S. Cambier, O. Ginis, S.J. Moreau, P. Gayral, J. Hearn, G. Stone, D. Giron, E. Huguet, J.M. Drezen, Gall
768 wasp transcriptomes unravel potential effectors involved in molecular dialogues with oak and rose
769 bushes. Front. Physiol., 10 (2019), 926.
770 [64] J.S. Ramsey, A.C.C. Wilson, M. de Vos, Q. Sun, C. Tamborindeguy, A. Winfield, G. Malloch, D.M.
771 Smith, B. Fenton, S.M. Gray, G. Jander, Genomic resources for *Myzus persicae*: EST sequencing, SNP
772 identification, and microarray design. BMC Genom., 8 (2007), 423–423.
773 [65] H. Boulain, F. Legeai, E. Guy, S. Morlière, N.E. Douglas, J. Oh, M. Murugan, M. Smith, J. Jaquiéry, J.
774 Peccoud, F.F. White, J.C. Carolan, J.-C. Simon, A. Sugio,. Fast evolution and lineage-specific gene family
775 expansions of aphid salivary effectors driven by interactions with host-plants. Genome Biol. Evol., 10
776 (2018), 1554-1572.
777 [66] J.C. Carolan, D. Caragea, K.T. Reardon, N.S. Mutti, N. Dittmer, K. Pappan, F. Cui, M. Castaneto, J.

778 Poulain, C. Dossat, D. Tagu, J.C. Reese, G.R. Reeck, T.L. Wilkinson, O.R. Edwards, Predicted effector
779 molecules in the salivary secretome of the pea aphid (*Acyrthosiphon pisum*): a dual
780 transcriptomic/proteomic approach. J. Proteome Res., 10 (2011), 1505–1518.
781 [67] C. Testerink, T. Munnik, Phosphatidic acid: a multifunctional stress signaling lipid in plants. Trends
782 Plant Sci., 10 (2005), 368-375.
783 [68] H.W. Xue, X. Chen, Y. Mei, Function and regulation of phospholipid signalling in plants. Biochem. J.,
784 421 (2009), 145–156.
785 [69] E.O. Martinson, J.D. Hackett, C.A. Machado, A.E. Arnold, Metatranscriptome analysis of fig flowers
786 provides insights into potential mechanisms for mutualism stability and gall induction. PloS One, 10
787 (2015), e0130745.
788 [70] I. Morkunas, V.C. Mai, B. Gabryś, Phytohormonal signaling in plant responses to aphid feeding. Acta
789 Physiol. Plant., 33 (2011), 2057–2073.
790 [71] P.I. Kerchev, B. Fenton, C.H. Foyer, R.D. Hancock, Infestation of potato (*Solanum tuberosum* L.) by
791 the peach-potato aphid (*Myzus persicae* Sulzer) alters cellular redox status and is influenced by
792 ascorbate. Plant Cell Environ, 35 (2012), 430-440.
793 [72] J. Louis, J. Shah. *Arabidopsis thaliana—Myzus persicae* interaction: shaping the understanding of
794 plant defense against phloem-feeding aphids. Front. Plant Sci., 4 (2013), 213.
795 [73] B. Favery, M. Quentin, S. Jaubert-Possamai, P. Abad. Gall-forming root-knot nematodes hijack key
796 plant cellular functions to induce multinucleate and hypertrophied feeding cells. J. Ins. Physiol., 84
797 (2016), 60-69
798 [74] A. Mine, C. Seyfferth, B. Kracher, M.L. Berens, D. Becker, K. Tsuda, The defense phytohormone
799 signaling network enables rapid, high-amplitude transcriptional reprogramming during effector-triggered
800 immunity. Plant Cell, 30 (2018), 1199-1219.
801 [75] L. Wu, H. Chen, C. Curtis, Z.Q. Fu, Go in for the kill: How plants deploy effector-triggered immunity to

802 combat pathogens. Virulence, 5 (2014), 710-721.

803 [76] K. Kazan, R. Lyons, Intervention of phytohormone pathways by pathogen effectors. Plant Cell, 26
804 (2014), 2285-2309.

805 [77] J.E. Park, J.Y. Park, Y.S. Kim, P.E. Staswick, J. Jeon, J. Yun, S.-Y. Kim, J. Kim, Y.-H. Lee, C.M. Park. GH3-
806 mediated auxin homeostasis links growth regulation with stress adaptation response in *Arabidopsis*. J.
807 Biol. Chem., 282 (2007), 10036–10046.

808 [78] B. Jones, S.A. Gunnerås, S.V. Petersson, P. Tarkowski, N. Graham, S. May, K. Dolezal, G. Sandberg, K.
809 Ljung, Cytokinin regulation of auxin synthesis in *Arabidopsis* involves a homeostatic feedback loop
810 regulated via auxin and cytokinin signal transduction. Plant Cell, 22 (2010), 2956-2969.

811 [79] G.E. Schaller, A. Bishopp, J.J. Kieber, The yin-yang of hormones: cytokinin and auxin interactions in
812 plant development. Plant Cell, 27 (2015), 44-63.

813 [80] J.A. O'Brien, E. Benková, Cytokinin cross-talking during biotic and abiotic stress responses. Front
814 Plant Sci., 4 (2013), 451.

815 [81] A. Karczmarek, H. Overmars, J. Helder, A. Goverse, Feeding cell development by cyst and root-knot
816 nematodes involves a similar early, local and transient activation of a specific auxin-inducible promoter
817 element. Mol. Plant Pathol., 5 (2004), 343-346.

818 [82] F.L. Goggin, Plant–aphid interactions: molecular and ecological perspectives. Curr. Opin. Plant Biol.,
819 10 (2007), 399-408.

820 [83] S. Luo, W. Hu, Y. Wang, B. Liu, H. Yan, Y. Xiang, Genome-wide identification, classification, and
821 expression of phytocyanins in *Populus trichocarpa*. Planta, 247 (2018), 1133-1148.

822 [84] M.-A. Cannesan, E. Nguema-Ona, Arabinogalactan proteins in root–microbe interactions. Trends
823 Plant Sci. 18 (2013) 440–449.

824 [85] J. Hearn, M. Blaxter, K. Schönrogge, J.L. Nieves-Aldrey, J. Pujade-Villar, E. Huguet, J.-M. Drezen, J.D.
825 Shorthouse, G.N. Stone, Genomic dissection of an extended phenotype: Oak galling by a cynipid gall
826 wasp. PLoS Gen. 15 (2019).

827 Figure 1: Gene Ontology treemap for the salivary transcriptome of *Phloeomyzus passerinii*. The box size
828 correlates to the number of sequences isolated. Numbers between brackets indicate the number of
829 sequences identified. Green boxes indicate binding proteins, purple boxes indicate enzymes, red boxes
830 indicate structural constituents, the blue box indicates transporters and the brown box molecular
831 transducers. The treemap was created with the treemap() function in R. A Detailed list of the proteins
832 can be found in the table S4.
833

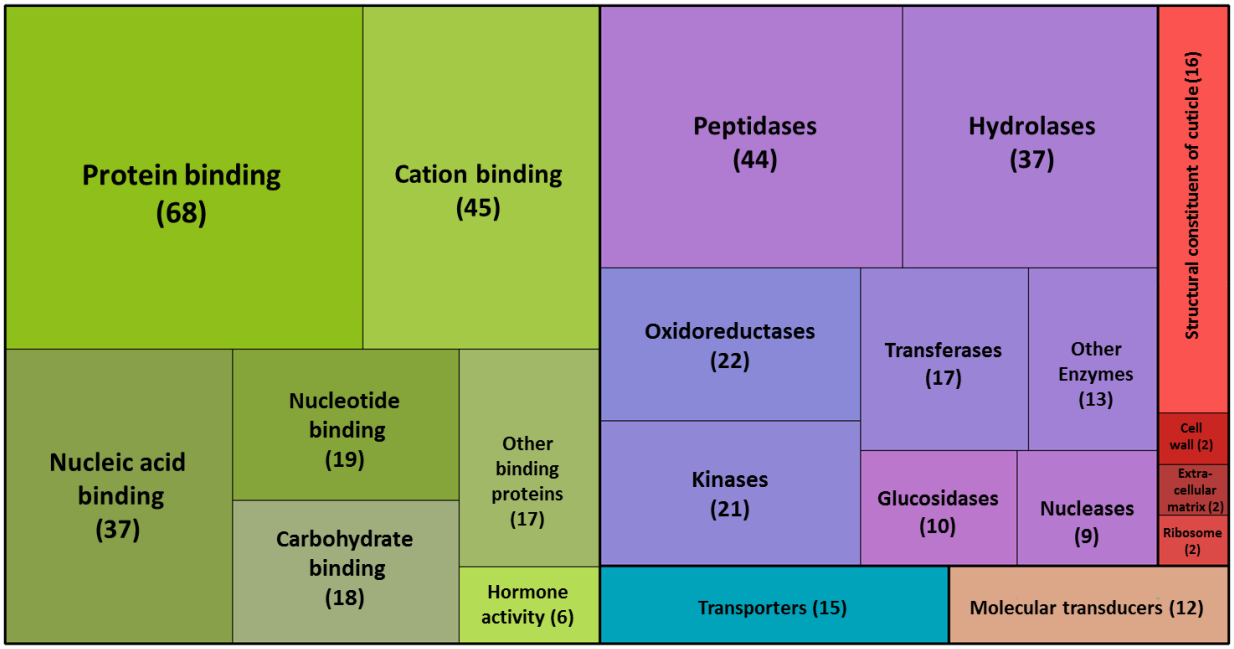

834
835

836 Figure 2: Representative salivary sheaths secreted in artificial diets by *Phloeomyzus passerinii*. Sheaths
837 stained and observed after 24 h probing in an agarose diet: (A) sheath stained with Coomassie blue; (B)
838 black stained sheaths in diet containing 0.1% DOPA, indicating a phenoloxidase activity, note the dark
839 halo surrounding the upper sheath; (C) reddish stained sheath in diet immersed with 0.1% DAB and 0.1%
840 H_2O_2, indicating a peroxidase activity. Black bars represent 10 µm.

841

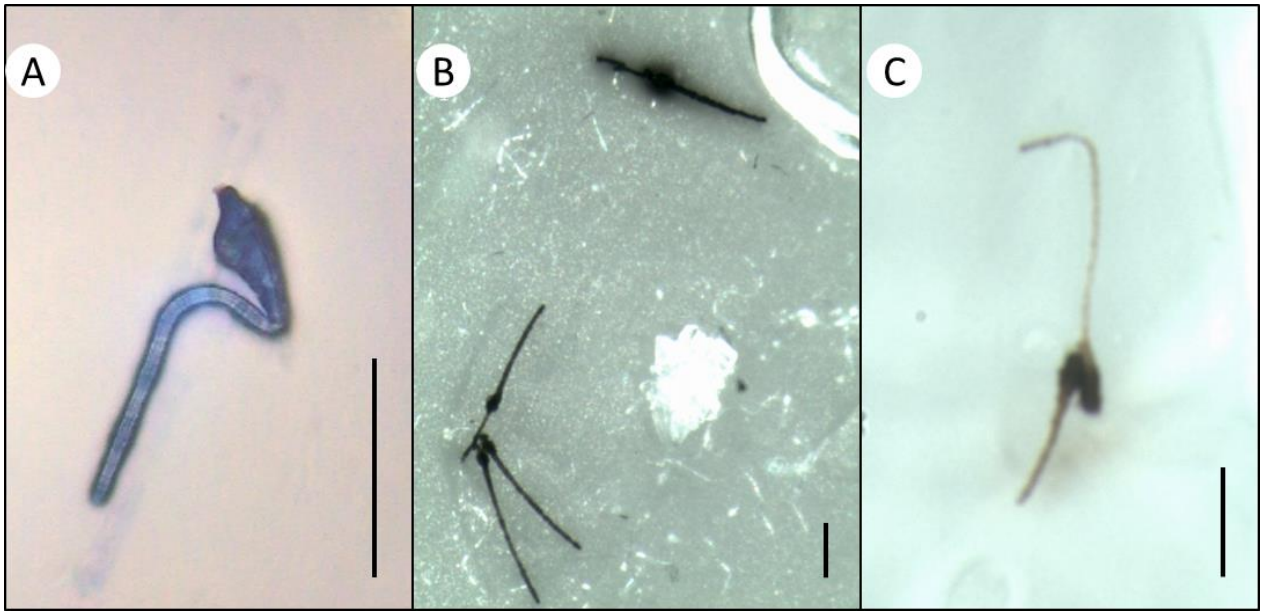

842

843

Figure 3: Heatmap of log_2-fold changes of 43 poplar genes belonging to eight different physiological processes or metabolic pathways (lower left box), after incubation of poplar protoplasts of two poplar genotypes (Koster and I-214) with salivary proteins of two aphids (*Myzus persicae* (*M. pers.*) and *Phloeomyzus passerinii* (*P. pass.*)). Non-host species interactions are expected between both poplar genotypes and *M. persicae*. Poplar is a host plant for *P. passerinii* but Koster is a resistant genotype while I-214 is a susceptible genotype. Downregulation appears in blue and upregulation in red. Gene code is presented below the heatmap, modalities (i.e. aphid x poplar genotype combinations are presented on the right of the heatmap). Hierarchical clustering was built with distances based on Pearson correlations. Approximately unbiased p-values (%) are indicated for the hierarchical clustering of modalities, red boxes indicate significant clusters at α = 0.05.

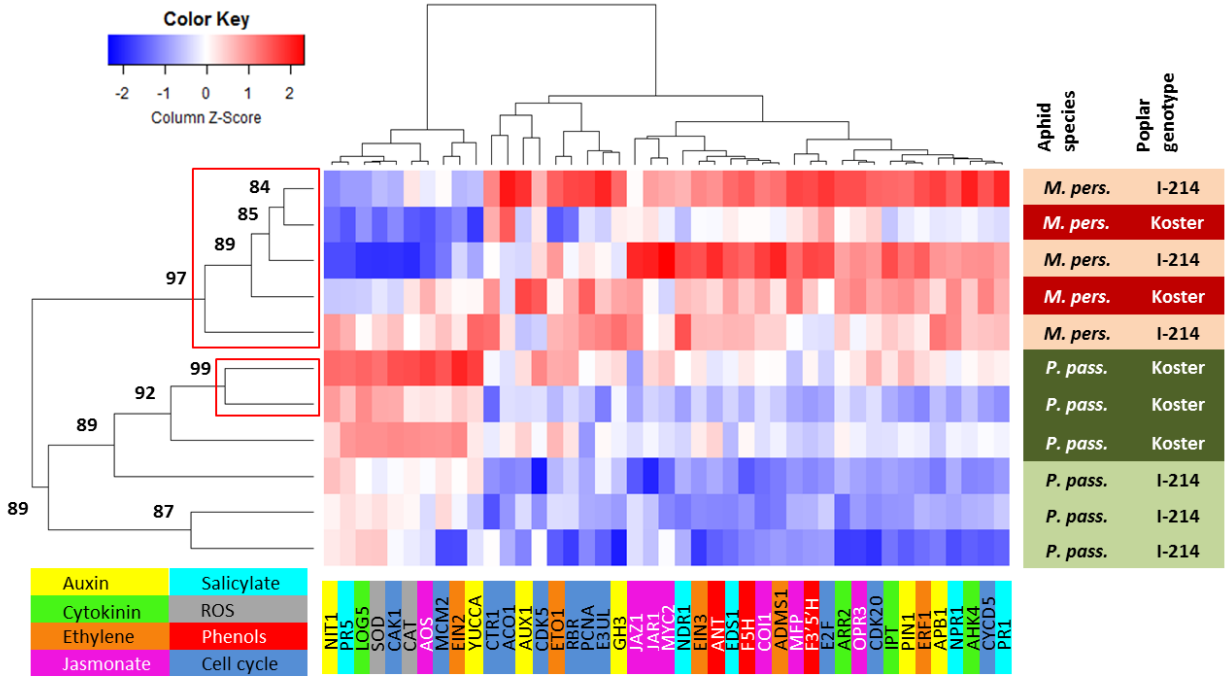

856 Figure 4: Mean (± SE) log_2-fold changes of genes involved in auxin (left) and cytokinin (right) pathways of
857 poplar protoplasts collected from two poplar genotypes (I-214 and Koster), after incubation with salivary
858 proteins of two aphids (*Myzus persicae* and *Phloeomyzus passerinii*), resulting in resistant or susceptible
859 interactions with a host species or non-host species interactions. Stars indicate modalities for which a
860 significant upregulation or downregulation of gene expression vs. controls was observed, using $^{\Delta}$Ct
861 values (t-test). ***, ** and * indicate a significant effect with P < 0.001, P < 0.01 and P < 0.05,
862 respectively. Different letters indicate significantly different groups (Tukey test) of log_2-fold changes
863 among modalities, for each gene.
864

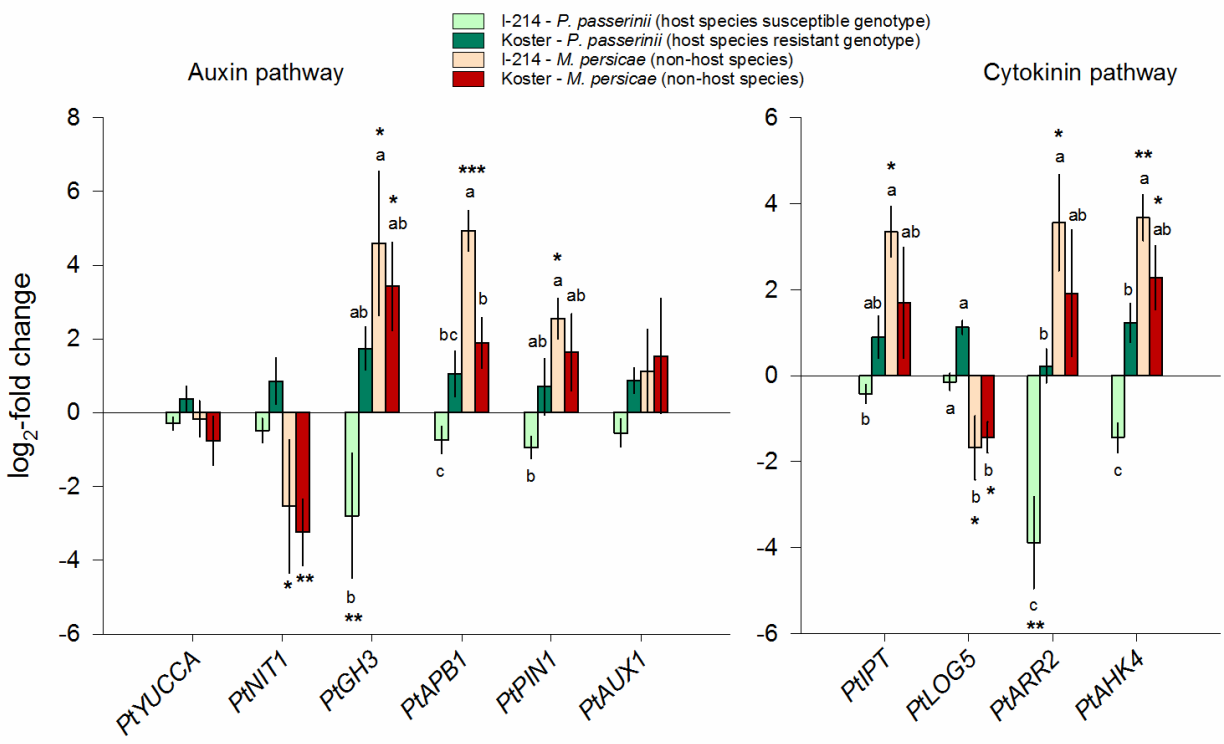

865
866

867 Figure 5: Mean (± SE) log_2-fold changes of genes involved in jasmonate, salicylic acid, ethylene pathways,
868 ROS responses and phenolic compounds of poplar protoplasts collected from two poplar genotypes (I-
869 214 and Koster), after incubation with salivary proteins of two aphids (*Myzus persicae* and *Phloeomyzus*
870 *passerinii*), resulting in resistant or susceptible interactions with a host species or non-host species
871 interactions. Stars indicate modalities for which a significant upregulation or downregulation of gene
872 expression vs. controls was observed, using $^{\Delta}$Ct values (t-test). ***, ** and * indicate a significant effect
873 with P < 0.001, P < 0.01 and P < 0.05, respectively. Different letters indicate significantly different groups
874 (Tukey test) of log_2-fold changes among modalities, for each gene.

875

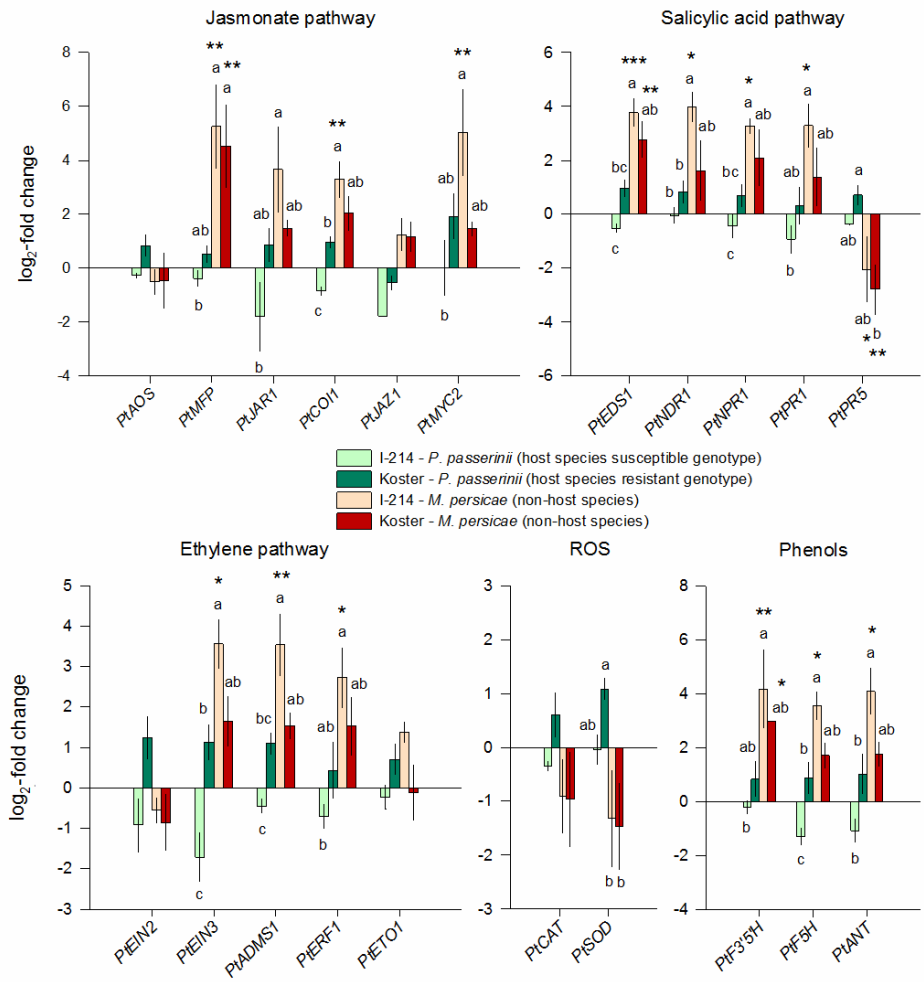

876

877 Figure 6: Mean (± SE) log_2-fold changes of genes involved in cell-division cycle of poplar protoplasts
878 collected from two poplar genotypes (I-214 and Koster), after incubation with salivary proteins of two
879 aphids (*Myzus persicae* and *Phloeomyzus passerinii*), resulting in resistant or susceptible interactions
880 with a host species or non-host species interactions. Stars indicate modalities for which a significant
881 upregulation or downregulation of gene expression vs. controls was observed, using $^{\Delta}$Ct values (t-test).
882 ** and * indicate a significant effect with P < 0.01 and P < 0.05, respectively. Different letters indicate
883 significantly different groups (Tukey test) of log_2-fold changes among modalities, for each gene.
884

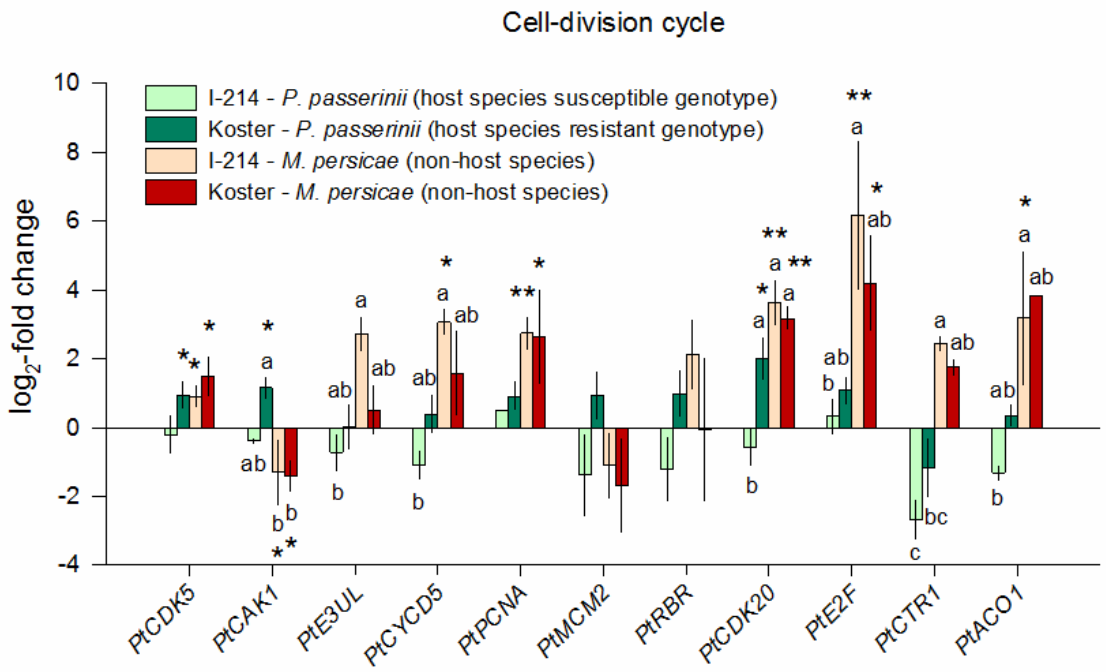

885

886 Figure 7: Representative GUS assays of transgenic seedlings of *Arabidopsis thaliana pIAA2*::GUS, showing
887 whole plants (A, C, E, G, I and K), and root tips (B, D, F, H, J and L), after 3 h of incubation in 20 µM of IAA
888 (A and B), TE/Tween buffer (C and D), and 1 and 10 µg of salivary proteins of *Phloeomyzus passerinii* (E, F,
889 I and J) or *Myzus persicae* (G, H, K and L). Black bars represent 1 mm for whole plants (A, C, E, G, I and K)
890 and 10 µm for root tips (B, D, F, H, J and L). Five seedlings were used for each modality.
891

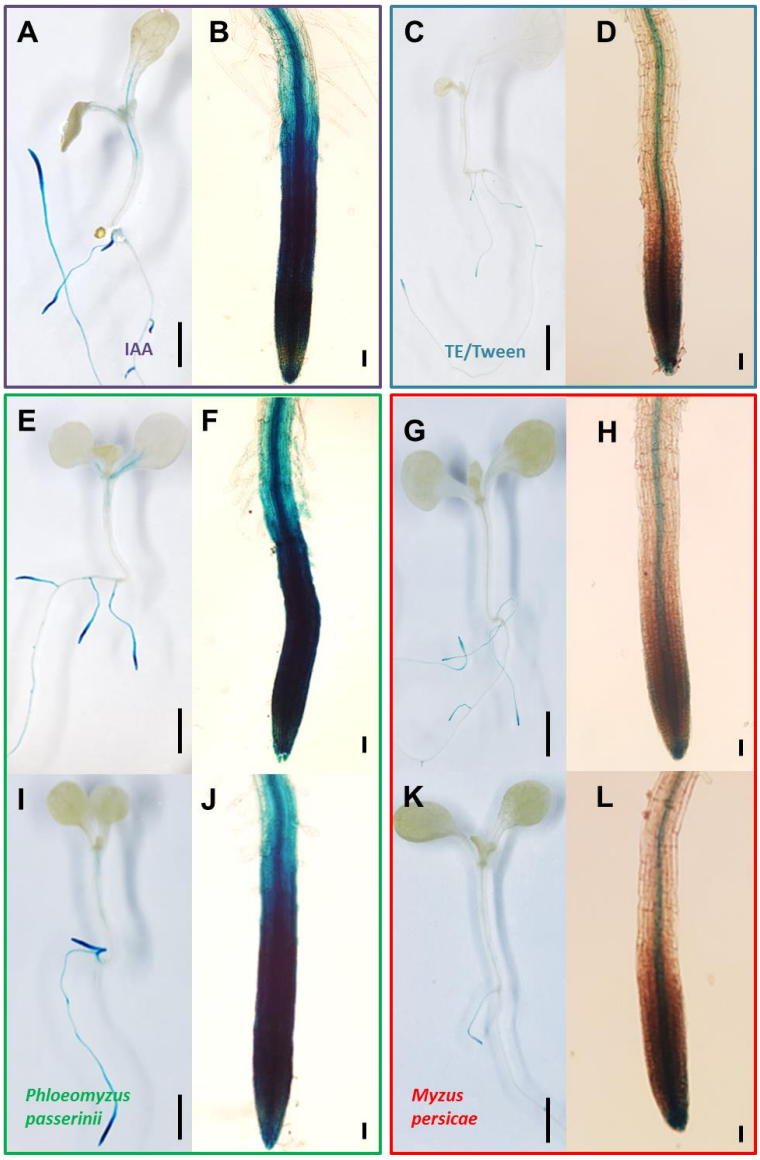

892
893

894 Figure 8: Representative GUS assays of transgenic seedlings of *Arabidopsis thaliana pARR16*::GUS,
895 showing whole plants (A, C, E, G, I and K), and root tips (B, D, F, H, J and L), after 4 h of incubation in 20
896 µM of BAP (A and B), TE/Tween buffer (C and D), and 1 and 10 µg of salivary proteins of *Phloeomyzus*
897 *passerinii* (E, F, I and J) or *Myzus persicae* (G, H, K and L). Black bars represent 1 mm for whole plants (A,
898 C, E, G, I and K) and 10 µm for root (B, D, F, H, J and L). Five seedlings were used for each modality.

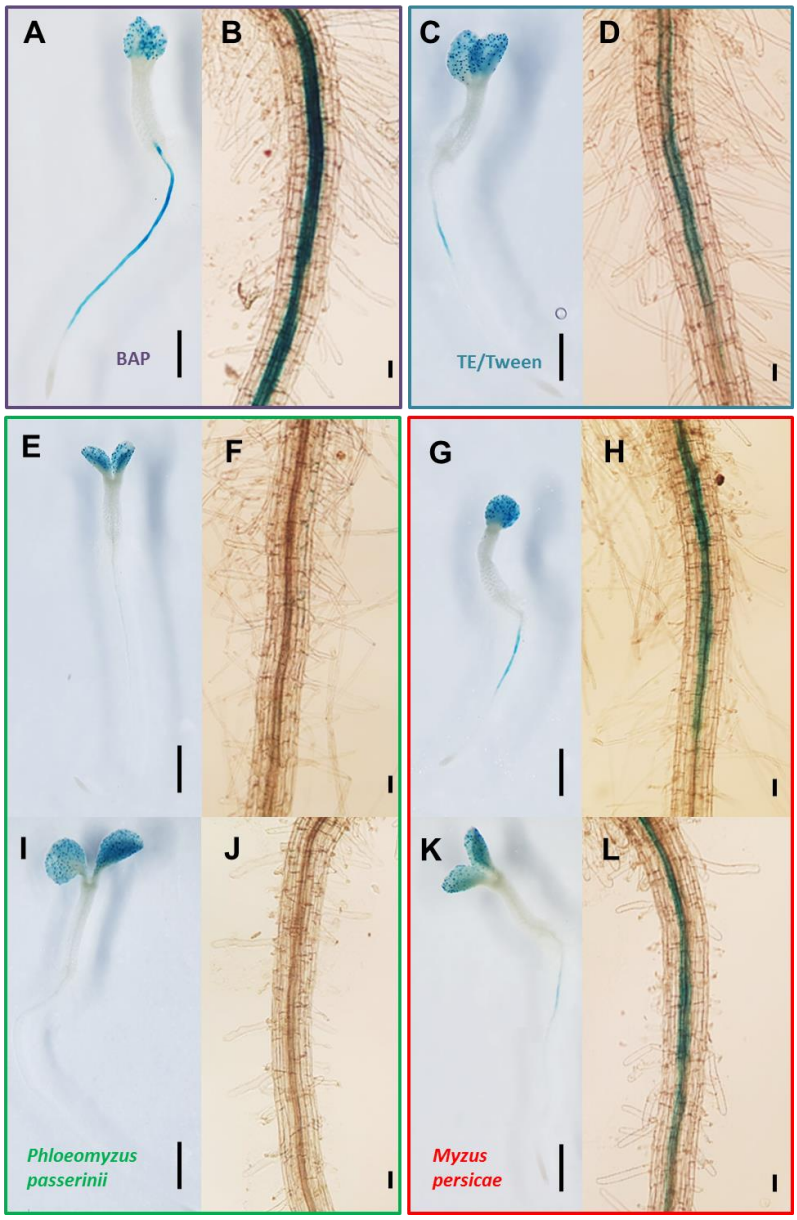

899

900 Figure 9: Graphical summary of effects of salivary extracts of *Phloeomyzus passerinii* on gene expression

901 in auxin and cytokinin pathways during a compatible interaction based on observations with *in vivo* RT-

902 qPCR assays with protoplasts (bold green) and heterologous *in planta* assay (bold orange).

903

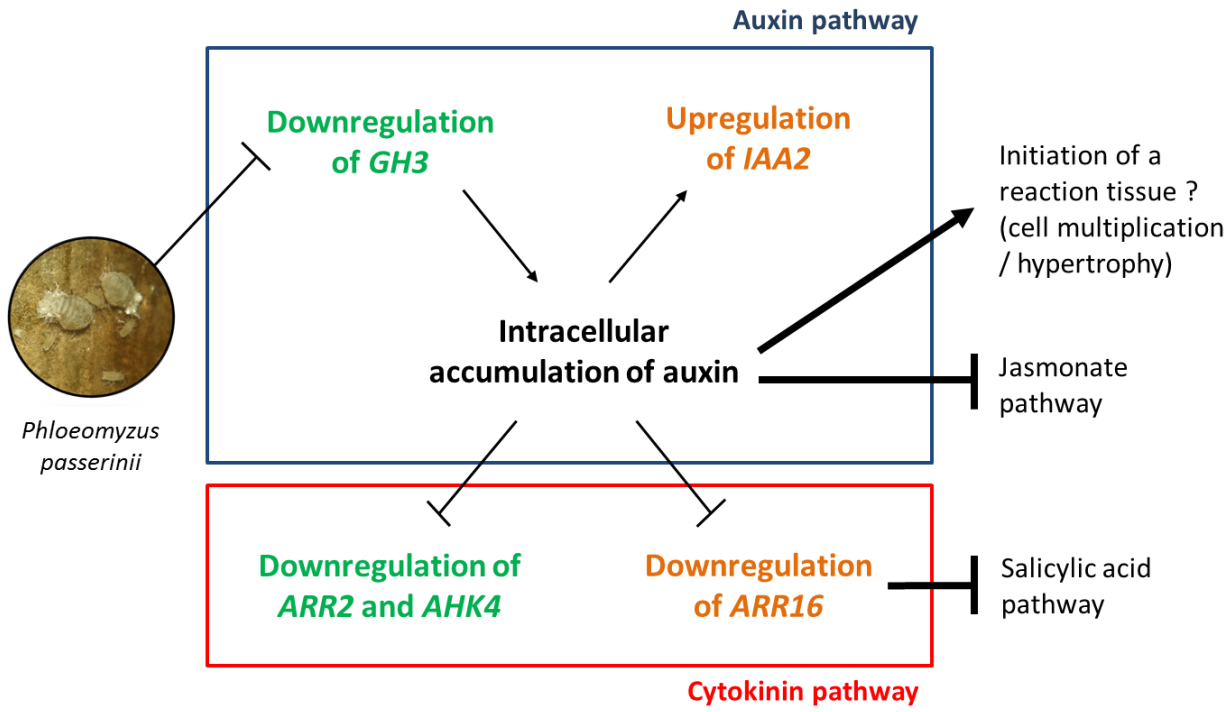

904

905 **Appendices**

906

907 Table S1: Illumina MiSeq sequencing and assembly statistics for *Phloeomyzus passerinii* salivary

908 transcriptome.

Number of raw read-pairs	15,453,942
Number of read-pairs after quality check*	11,578,269
Number of assembled transcripts	36,312
Average transcript length (bases)	858
N50 (bases)	1273
Transcriptome completeness (%)**	86.0 complete + 4.4 partial

909 * the reads were quality-clipped before performing the assembly with Trimmomatic v0.32. (Bolger *et al.* 2014).

910 ** assessed on 1066 core genes

911 Table S2: Genes considered for RT-qPCR, their sequence code in Phytozome and primers sequences.

Physiological process	Gene code	Sequence code	Protein	Primer fwd sequence	Primer rev sequence	Amplicon length	Tm	GC (%)	Optimal annealing temperature
Auxin	APB1	POPTR_ 0013s04160	Actin-binding protein ABP140	TCGTTTCCACCCATTCT TCTGTG	CACCACCCTCTTTAACAT CTGAGG	128	61.3	48.9	60.3
Auxin	PIN1	POPTR_ 0007s14010	Peptidyl-prolyl cis-trans isomerase NIMA-interacting 1	GGGACTCAAGTTCGA GCATCACAC	TGGGTCTTTCCATGATGC CTTCC	75	63.6	53.2	60.1
Auxin	YUCCA	POPTR_ 0005s20840	Indole-3-pyruvate monoxygenase YUCCA11-related	CTGTACTGGATTGGCT GAAGGATG	CAGCACAGTAAAGCCCA TTTCCC	65	61.7	47.9	58.2
Auxin	GH3	POPTR_ 0003s15970	Auxin-responsive GH3 family protein	GCCTTCGACTGCTGAA GAATTGG	TGGTCCAAGCCATCAAC ATACTTG	90	62.2	49.0	58.4
Auxin	AUX1	POPTR_ 0005s16020	Auxin influx carrier (AUX1 LAX family)	TGGCATGGTGGTTCAG TATGTG	TGAGAAGCACTTGTGCA ACCTG	65	61.8	50.0	59.4
Auxin	NIT1	POPTR_ 0004s21160	Nitrilase-like protein 1	TGGTCTCCGCTCTCCA ATTTGC	AGCAGCTCTAACCAATCT TTCAGC	80	62.6	50.2	61.4
Cytokinin	IPT	POPTR_ 0014s13540	TRNA delta 2 - isopentenylpyrophosphate transferase related	AGCAGAGCATGCCTG GGAAATG	AGAGGAGTTGTCCCACA ATGGC	65	63.4	54.5	62.1
Cytokinin	AHK4	POPTR_ 0010s11350	Histidine kinase 4	GTGCTGACAGTGGTA AAGAAGCAC	GATACGACGTGTAGCCT CAAACCC	114	62.7	52.3	60.8
Cytokinin	LOG5	POPTR_ 0004s18850	Cytokinin riboside 5' - monophosphate PHOSPHORIBOHYDROLASE LOG5	TCTGCACCAAGTGCCA AAGAACTC	ATCATGCACAGGCACGT ACTCCTC	60	64.6	52.1	59.0
Cytokinin	ARR2	POPTR_ 0014s12030	RESPONSE REGULATOR OF TWO-COMPONENT SYSTEM	GAAATGGATTTGCCTG TCGTCATC	AGCACCCTGAAGAACAC CCTTC	78	62.0	50.2	58.1
Cell cycle	CDK5	POPTR_ 0006s05850	CDK5 REGULATORY SUBUNIT-ASSOCIATED PROTEIN 3	TTCATCATGGCCAAAG CAGGAAG	CATCAAACATGGACGAG AGTGTCC	79	62.5	51.0	60.8
Cell cycle	CAK1	POPTR_ 0018s09000	Pt-CAK1.2	AGCCTGCCTCCCTAAT CATTCC	AGCTGGGTCATAGCAGA CAAGC	70	62.6	54.5	60.8
Cell cycle	E3UL	POPTR_ 0003s20350	E3 UBIQUITIN LIGASE BIG BROTHER	ACTTGAATTAGGCGAG ACAGTTGG	TGGCAAATGACACACCT CTCAC	138	61.4	47.9	60.8
Cell cycle	CYCD5	POPTR_ 0014s01700	CYCLIN-D5-1	GGCTAATCGAGAGCCT CATCAAGG	CAAGCGGGCAGTTCTAA ACGAG	79	62.8	54.4	59.5
Cell cycle	PCNA	POPTR_ 0001s25490	PROLIFERATING CELL NUCLEAR ANTIGEN	ACACCACAGTTGATAA GCCGGAAG	GAAGGAGTTCATGTACC TCAGTGC	62	62.9	50.0	59.2
Cell cycle	MCM2	POPTR_ 0006s02620	MINICHROMOSOME MAINTENANCE (MCM2/3/5) FAMILY PROTEIN	AGGAATAAACCCAATT CCCAACGC	AGTGTGCTTCCCTCTACC ACTTC	77	62.8	49.0	60.0
Cell cycle	RBR	POPTR_ 0001s06870	RETINOBLASTOMA-ASSOCIATED PROTEIN RB –RELATED	TGCTGGTGGATGTTGG TTCTGC	AGGTGATGCAGGACATT GACCATC	95	63.7	52.3	60.3
Cell cycle	CDK20	POPTR_ 0091s00250	CYCLIN-DEPENDENT KINASE 20	TGGAGATAAGCTGGT GCTCACTG	CCTATACGCAATGGTAGT GACCTG	97	61.9	51.1	61.6
Cell cycle	E2F	POPTR_ 0015s08160	E2F TRANSCRIPTION FACTOR-LIKE E2FE	ATCTCACTCGATGAAT CTGCCAAG	CTTGTATCAGCAGTGTG GGTCTTC	146	61.4	47.9	60.2

912

913

914

915

916

917

918

919 Table S2 cont.

Physiological process	Gene code	Sequence code	Protein	Primer fwd sequence	Primer rev sequence	Amplicon length	Tm	GC (%)	Optimal annealing temperature
Ethylene	CTR1	POPTR_0016s11050	serine/threonine-protein kinase CTR1	TGAGTCTTGCTGGGCCAATGAAC	TCATGCCTGCAAGACCAGGTTG	113	63.8	53.4	63.0
Ethylene	ACO1	POPTR_0004s00460	Aminocyclopropanecarboxylate oxidase	TGGAGGTGATCAATGATGCCTGTG	ATCCCATGGTTCACCAACTCAAAG	60	62.4	48.9	58.7
Ethylene	EIN3	POPTR_0001s05360	ETHYLENE-INSENSITIVE3-like 3 protein	AACTGCAGCGCAACCATTTCTG	ACAACTGTTAAGGCAGCACCTC	74	62.3	50.0	58.9
Ethylene	ADMS1	POPTR_0014s11000	S-adenosylmethionine synthetase 1	TCGTAGGTGCATTGTGCAAGTC	TGCCATAGGTGTCCACAAAGACAG	79	62.5	50.0	60.8
Ethylene	ERF1	POPTR_0001s36610	Ethylene responsive element binding factor 3	CTTCTTCTTTGTGCCGCAAGCC	ATCACCAGAGCCCAAGTCAACC	80	63.2	54.5	61.3
Ethylene	EIN2	POPTR_0016s09210	ethylene-insensitive protein 2	TAAGCGAGGAGAGTGTGTTTGCC	ATTTGGTGGTCCCTGATGTTGCAG	109	63.6	52.2	61.7
Ethylene	ETO1	POPTR_0016s13180	ETO1-LIKE PROTEIN 2-RELATED	CTCTATAAGAGAGCACGGGAACGG	TTTCCCTGAGGAACACTGGCTCTC	67	63.6	54.2	59.6
Jasmonic acid	AOS	POPTR_0004s15600	allene oxide synthase	TGAACCTCCGGTTCCATTCCAG	ATAGGCCGCGTGATGACTTTCG	73	63.1	54.5	61.0
Jasmonic acid	JAZ1	POPTR_0001s16640	jasmonate ZIM domain-containing protein	TGAAGCGCCTAACGGTTCAGATG	GGAGAAGAACCGATGAAGTGATGC	64	62.9	51.1	59.8
Jasmonic acid	MFP	POPTR_0010s01570	MULTIFUNCTIONAL PROTEIN	GGAAGGAAGCAGGACTAAGGGAAG	GTCCTTCAAGCTGTACAACACGTC	124	62.6	52.1	61.9
Jasmonic acid	JAR1	POPTR_0014s09120	jasmonic acid-amino synthetase	GAGTGTTGCAATTGCCTGGATCG	ATGGCCTTCACCTTCCGTGAAC	71	63.3	53.4	60.6
Jasmonic acid	MYC2	POPTR_0002s17750	transcription factor MYC2	CGTGAACAGAAGAACGCTCGTG	AAGACAGGCCTGGTTTATTAGCG	70	62.0	51.2	58.1
Jasmonic acid	COI1	POPTR_0008s06460	CORONATINE INSENSITIVE 1	AGCACTTCCGCTCTAGGTACAC	AGGTTAAGCTAACTGCCACAGACG	61	62.7	52.3	58.8
Jasmonic acid	OPR3	POPTR_0018s07120	12-oxophytodienoate reductase	ACAAGATGTAGGGCGTTGAATGGG	TTCCAGGCACATGAGGAAACCC	142	63.4	52.3	65.7
Phenolics	F3’5’H	POPTR_0007s06300	Flavonoid 3',5'-hydroxylase / F3'5'H	GCTGCGAAGCATATCTCTTACGTG	ACGCATGCCCTCATGAATCAC	139	62.4	52.3	61.6
Phenolics	ANT	POPTR_0001s40590	Anthocyanin 5-O-glucoside 6'''-O-malonyltransferase	AAGTCGTTTAGACCCTCCTCTTCC	ATGTGACGAGCCACAACAGTATC	63	61.6	48.9	57.9
Phenolics	F5H	POPTR_0007s13720	ferulate-5-hydroxylase	TGATGTTTGGTGGGACAGAGACG	TCTTCATTAGCTCCGCCATGACC	66	63.0	52.2	61.6
ROS	SOD	POPTR_0005s09190	SUPEROXIDE DISMUTASE	GATTTCAACAATGCTGCCCAGGTC	TGCCAAGTTCTGGCATGTCTCC	66	62.7	51.1	57.8
ROS	CAT	POPTR_0005s27300	CATALASE 3	TTCTGCTGTCTGCAGTGGAAGG	CGAACGAAACGTTCTTGCCTGTC	113	62.9	54.5	62.9
Salicylic acid	PR1	POPTR_0001s29530	Pathogenesis-related protein	CTACGTCAATGCCCACAATAATGC	CTGCCACATTAGTGTCCCAGAC	74	61.2	50.2	59.6
Salicylic acid	EDS1	POPTR_0015s08100	ENHANCED DISEASE SUSCEPTIBILITY 1	GAATGACCTAGGCCTGAGTGAAAG	TTCTCTAACGCTTCAGCAGCAC	63	61.4	50.0	59.7
Salicylic acid	NPR1	POPTR_0014s11120	NPR1 interacting (NPR1_interact)	CCCTGCATACAACAACCAACAAC	TCGCGAATGCCCTTGATGAG	137	61.2	51.4	60.2
Salicylic acid	PR5	POPTR_0005s26240	receptor serine/threonine kinase PR5K	ACAGCTACACACCACTCGTCAAC	AGATGGCGATGCTCCATTCTGG	71	63.4	53.4	60.6
Salicylic acid	NDR1	POPTR_0012s12790	NDR1/HIN1-LIKE	GCAACAACTGCAGGCTGGAATC	AGCTTGATTCTCACAGGCTGGTC	62	62.9	54.5	60.2

920

921

922 Table S3: Number of orthologous proteins between the salivary transcriptomes of *Phloeomyzus*

923 *passerinii* and *Myzus persicae.*

Proteins	***P. passerinii***	***M. persicae***
Ejaculatory bulb-specific protein 3	1	3
Chorion peroxidase	5	2
Cathepsin B-like cysteine proteinase 4	5	1
esterase E4-like isoform X1	5	1
carbonic anhydrase 7-like	3	1
Collagen alpha-1(IV) chain	2	1
cathepsin D	2	1
Vitellogenin-1	2	1
Protein takeout	1	1
15 kDa seleno -like precursor	1	1
Probable sodium/potassium/calcium exchanger CG1090	1	1
Phosphatidylethanolamine-binding protein homolog F40A3.3	1	1
Neuroglian	1	1
Cuticle protein 18.6, isoform B	1	1
WD repeat-containing 18	1	1
transmembrane emp24 domain-containing eca	1	1
Translocon-associated protein subunit beta	1	1
PREDICTED: uncharacterized protein LOC100160421	1	1
phosphatidylinositol-4-phosphate 5-kinase	16	0
Glucose dehydrogenase [FAD, quinone]	8	0
Gut esterase 1	8	0
Serine protease	7	0
Furin-like protease	6	0
Transcription factor SPT20 homolog	6	0
Phospholipase A1	5	0
Probable serine/threonine-protein kinase nek3	5	0
cuticle precursor	4	0
Protein Toll	4	0
tyrosine kinase receptor	4	0
Acetylcholine receptor	3	0
Activating signal cointegrator 1 complex subunit 2 homolog	3	0
Down syndrome cell adhesion molecule-like protein Dscam2	3	0
Fibroin heavy chain	3	0
leucine-rich repeat containing G-coupled receptor	3	0
Peritrophin-1	3	0
zinc metallo ase nas-13-like	2	0
60S ribosomal protein L27a	2	0
AF4 FMR2 family member 4-like	2	0
Basement membrane proteoglycan	2	0
cell wall DAN4	2	0
C-type lectin-like precursor	2	0
Cuticle protein	2	0
Cuticle protein 19	2	0
Diuretic hormone	2	0
DNA-directed RNA polymerase II subunit RPB1-like	2	0
Dolichyldiphosphatase 1	2	0
endocuticle structural glyco bd-8-like	2	0
Endocuticle structural glycoprotein SgAbd-2	2	0
Endoglucanase	2	0

924

925 Table S3 cont.

Extensin	2	0
glia-derived nexin	2	0
Heterogeneous nuclear ribonucleoprotein A1	2	0
Hypertrehalosaemic prohormone	2	0
hypothetical protein WALSEDRAFT_31439	2	0
Low-density lipoprotein receptor-related protein	2	0
Maltase A2	2	0
mesencephalic astrocyte-derived neurotrophic factor homolog	2	0
multiple epidermal growth factor-like domains 10	2	0
Neurogenic locus Notch protein	2	0
Neuropeptide CCHamide-1	2	0
nose resistant to fluoxetine 6- partial; nose resistant to fluoxetine 6-like	2	0
odorant binding 10	2	0
odorant binding 9	2	0
PREDICTED: meteorin-like protein	2	0
PREDICTED: spondin-1-like	2	0
Probable G-protein coupled receptor Mth-like 1	2	0
probable serine threonine- kinase nek3	2	0
Protein yellow	2	0
proto-oncogene tyrosine- kinase ROS	2	0
Putative UDP-glucuronosyltransferase ugt-47	2	0
synaptic vesicular amine transporter isoform X1	2	0
Thioredoxin domain-containing protein	2	0
transmembrane emp24 domain-containing bai-like isoform X2	2	0
Transmembrane emp24 domain-containing protein A	2	0
uncharacterized family 31 glucosidase KIAA1161-like	2	0
Angiotensin-converting enzyme	1	0
Beta-amyloid-like protein	1	0
canopy homolog 4-like precursor	1	0
Cathepsin L	1	0
flocculation FLO11-like	1	0
prostatic spermine-binding -like	1	0
Protein 60A	1	0
Putative acid phosphatase 5	1	0
Slit homolog 1 protein	1	0
sulfhydryl oxidase 2-like	1	0
Translocon-associated protein subunit alpha	1	0

926

927 Table S4: Gene ontology annotations of genes from salivary glands of *Phloeomyzus passerinii*. All genes

928 belonged to the Molecular Function category.

Gene Ontology (GO)	Number of sequences
protein binding	55
nucleic acid binding	19
structural constituent of cuticle	16
phosphatidylinositol phosphate kinase activity	15
serine-type endopeptidase activity	15
zinc ion binding	13
chitin binding	13
DNA binding	13
metal ion binding	12
calcium ion binding	12
odorant binding	9
ATP binding	9
hydrolase activity	7
protein dimerization activity	7
hormone activity	6
oxidoreductase activity	6
cysteine-type endopeptidase activity	6
peroxidase activity	5
metalloendopeptidase activity	5
nucleotide binding	5
heme binding	5
carboxylic ester hydrolase activity	4
DNA-binding transcription factor activity	4
peptide-methionine (S)-S-oxide reductase activity	4
protein-hormone receptor activity	3
triglyceride lipase activity	3
nuclease activity	3
RNA binding	3
N-acetyltransferase activity	3
catalytic activity	3
transporter activity	3
acetylcholine-gated cation-selective channel activity	3
transferase activity, transferring hexosyl groups	3
hydrolase activity, hydrolyzing O-glycosyl compounds	3
peptidase activity	3
chitinase activity	3
metallopeptidase activity	3
aspartic-type endopeptidase activity	2
3'-5' exonuclease activity	2
serine-type endopeptidase inhibitor activity	2
hydrolase activity, acting on glycosyl bonds	2
oxidoreductase activity, acting on CH-OH group of donors	2
cellulase activity	2
leucine-tRNA ligase activity	2
structural constituent of cell wall	2
acid phosphatase activity	2
G-protein coupled receptor activity	2
heparin binding	2
scavenger receptor activity	2
sulfuric ester hydrolase activity	2
cation binding	2
protein tyrosine kinase activity	2
growth factor activity	2
transferase activity	2

929

930 Table S4 cont.

931

extracellular matrix structural constituent	2
transition metal ion binding	2
carbohydrate binding	2
obsolete signal transducer activity	2
cholinesterase activity	2
RNA-DNA hybrid ribonuclease activity	2
iron ion binding	2
aminoacyl-tRNA editing activity	2
serine-type peptidase activity	2
GTP binding	2
transferase activity, transferring glycosyl groups	2
flavin adenine dinucleotide binding	2
structural constituent of ribosome	2
G-protein beta/gamma-subunit complex binding	1
cysteine-type peptidase activity	1
mRNA binding	1
DNA-directed 5'-3' RNA polymerase activity	1
transmembrane receptor protein serine/threonine kinase activity	1
lysozyme activity	1
unfolded protein binding	1
omega peptidase activity	1
iron-sulfur cluster binding	1
alpha,alpha-trehalase activity	1
protein kinase binding	1
sequence-specific DNA binding	1
voltage-gated potassium channel activity	1
endopeptidase inhibitor activity	1
transmembrane transporter activity	1
protein kinase activity	1
copper ion binding	1
DNA-directed DNA polymerase activity	1
endonuclease activity	1
carboxypeptidase activity	1
O-acyltransferase activity	1
hedgehog receptor activity	1
isomerase activity	1
proton transmembrane transporter activity	1
GTPase activator activity	1
cis-stilbene-oxide hydrolase activity	1
carbonate dehydratase activity	1
metallocarboxypeptidase activity	1
cation transmembrane transporter activity	1
phosphatase activity	1
extracellular ligand-gated ion channel activity	1
cysteine dioxygenase activity	1
ion channel inhibitor activity	1
transmembrane receptor protein tyrosine kinase activity	1
protein heterodimerization activity	1
polysaccharide binding	1
G-protein coupled receptor binding	1
1-alkyl-2-acetylglycerophosphocholine esterase activity	1
sulfotransferase activity	1
ATPase activity, coupled to transmembrane movement of substances	1

932 Table S4 cont.

ubiquitin protein ligase binding	1
phospholipase A2 activity	1
poly(A)-specific ribonuclease activity	1
obsolete signal transducer, downstream of receptor, with serine/threonine kinase activity	1
glucosylceramidase activity	1
hydrolase activity, acting on carbon-nitrogen (but not peptide) bonds	1
ionotropic glutamate receptor activity	1
signaling receptor binding	1
GPI-anchor transamidase activity	1
extracellularly glutamate-gated ion channel activity	1
dolichyl-diphosphooligosaccharide-protein glycotransferase activity	1
thiol oxidase activity	1
phosphatidylinositol N-acetylglucosaminyltransferase activity	1
ion channel activity	1
oxidoreductase activity, acting on the aldehyde or oxo group of donors, NAD or NADP as acceptor	1
peptidyl-dipeptidase activity	1
FMN binding	1
electron transfer activity	1
lipid transporter activity	1
transferase activity, transferring acyl groups other than amino-acyl groups	1
beta-glucuronidase activity	1
alpha-mannosidase activity	1
GTPase activity	1
hydrolase activity, acting on carbon-nitrogen (but not peptide) bonds, in linear amides	1
protein serine/threonine kinase activity	1
succinate dehydrogenase activity	1
mannosyl-oligosaccharide 1,2-alpha-mannosidase activity	1

933 Figure S1: Pipeline for the annotation process. Data are in orange, analyses in blue, results in green.

934

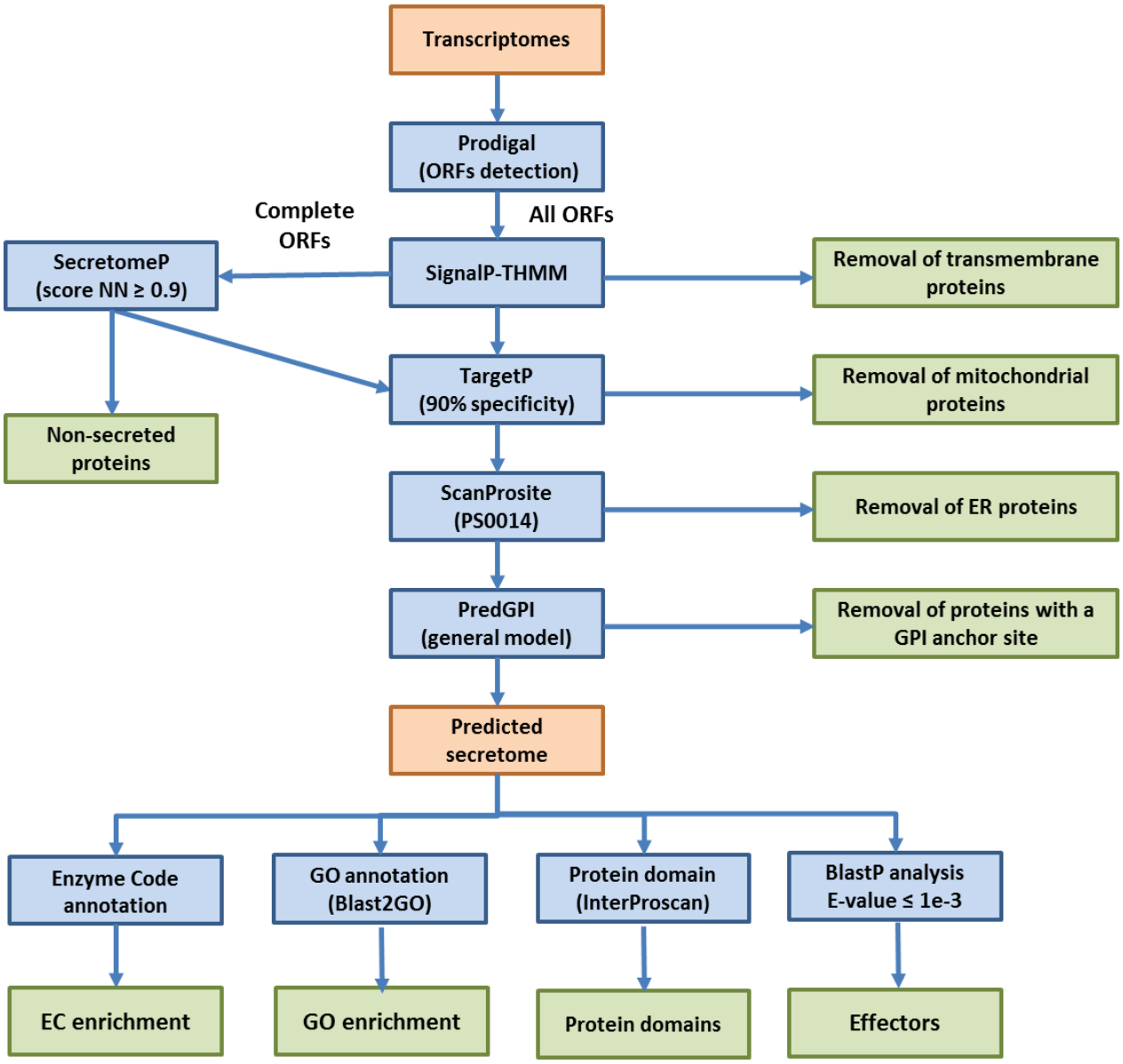

935

936

937 Fig. S2 Mean (± SE) log_2-fold changes of several poplar genes after incubation of I-214 poplar protoplasts

938 with different doses (1, 10, 20 , 40 and 80 µg) of salivary proteins of *Phloeomyzus passerinii* (upper

939 graph) and *Myzus persicae* (lower graph). Two biological replicates were performed for *P. passerinii* and

940 one for *M. persicae*.

941

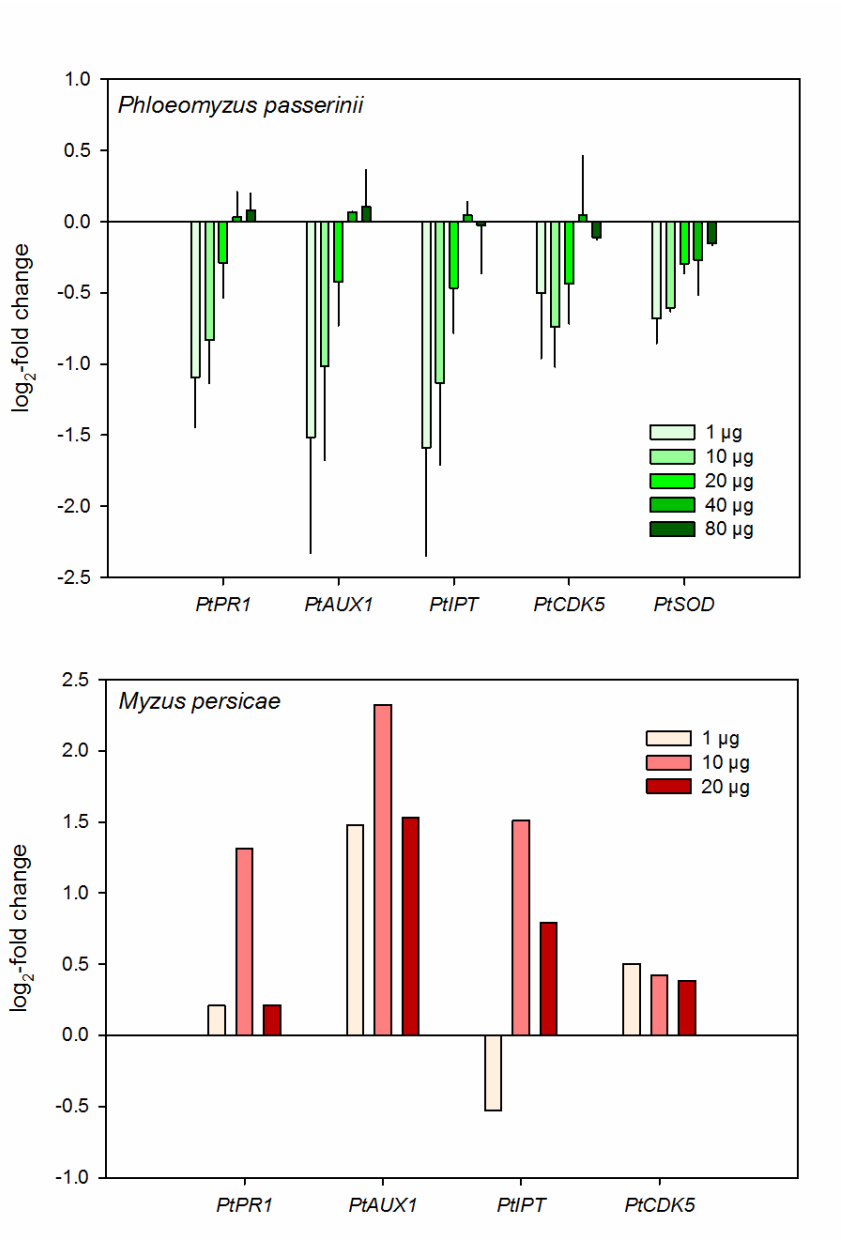

942

943 Fig. S3: FDA assay on poplar protoplasts after 3 h of incubation with salivary proteins of *Phloeomyzus*
944 *passerinii* (A, B) and *Myzus persicae* (C, D). Black bars represent 25 µm. Most protoplasts were
945 fluorescent after treatment, indicating that incubation with salivary proteins of aphids did not affect
946 their survival.

947

948 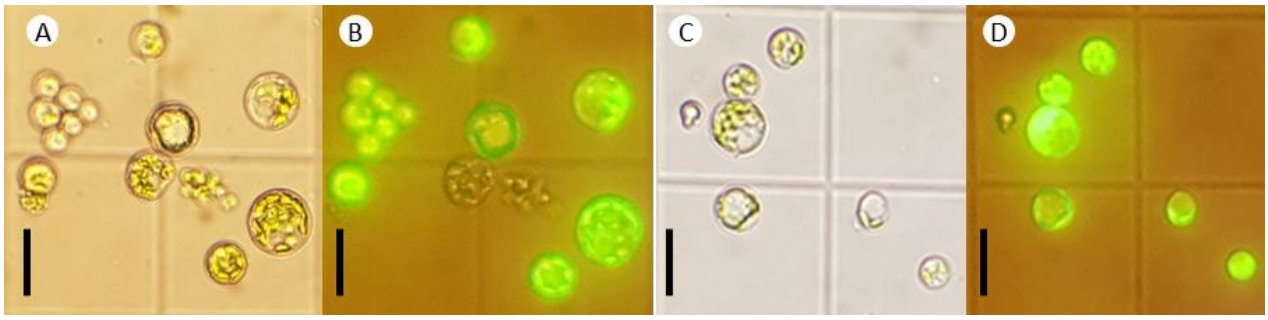

949